ACS Catalysis

pubs.acs.org/acscatalysis
Research Article

Expanding the "Terpenome": Diterpene Synthases Accept GGPP-Ether Substrates

Viktoria Ravkina, Gerald Dräger, Jörn Droste, Svenja Schwörer, Ahmed Hassanin, Mehdi D. Davari,* and Andreas Kirschning*

Cite This: ACS Catal. 2025, 15, 6796−6811
Read Online

ACCESS | Metrics & More | Article Recommendations | Supporting Information

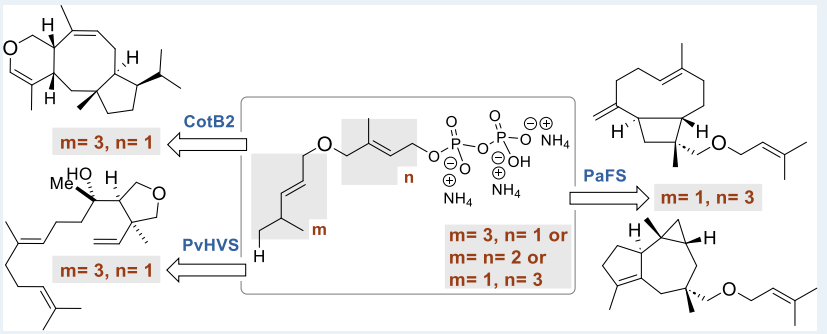

ABSTRACT: Three geranylgeranyl pyrophosphate derivatives carrying an ether group at different positions within geranylgeranyl pyrophosphate were employed in biotransformations with five diterpene synthases (CotB2, PvHVS, PaFS, Bnd4 and TXS) derived from plants, bacteria and fungi. A total of six new oxygen-containing diterpenoids were isolated and characterized, deepening our knowledge on the substrate promiscuity of diterpene synthases. In addition, the diterpene synthase PvHVS also accepts an ether derivative of farnesyl pyrophosphate and converts it to the same tetrahydrofuran core as found for the analogous extended GGPP substrate. This result further demonstrates that diterpene synthases also exhibit promiscuity toward truncated unnatural substrates.

KEYWORDS: *biotransformations, diterpene synthases, diterpenoids, farnesyl pyrophosphates, non-natural terpenes*

INTRODUCTION

Diterpene synthases (DTCs), like other terpene synthases (TCs), use linear, unsaturated, methyl-branched precursors. In the case of DTCs, this is geranylgeranyl pyrophosphate (GGPP, **1**), initially forming a more or less prominent cationic allyl intermediate that can react further with distant alkenes to form (oligo)carbocyclic products, the diterpenes.[1−3]

Investigations on the substrate promiscuity of sesquiterpene synthases (STCs) have increasingly become the focus of attention,[4−15] and only recently this has also been successfully extended to diterpene synthases by the Dickschat group.[16,17] They demonstrated that the GGPP isomers **7** and **8** are accepted by several DTCs, including cyclooctat-9-en-7-ol synthase (CotB2) (Scheme 1A). We showed that the insertion of an oxygen atom into the backbone of farnesyl pyrophosphate (FPP), the linear precursor of sesquiterpenes, allows conversion by STCs to yield new "oxy" sesquiterpenes with significantly altered and still complex backbone compared to the natural cyclization product. Due to the additional oxygen atom, they can exert olfactoric properties with value for the fragrance and aroma industries.[12] The cyclization mechanisms that lead to the new sesquiterpenoids do not necessarily follow the native mechanism, indicating that some STCs have the ability to adapt mechanistically in line with the structural features of the substrate.

We have expanded our research program to include diterpene synthases into the portfolio, and in particular we aim to use our experience gained from FPP ethers to generate ether-bearing diterpene derivatives.[15] Here we report on initial investigations to transform three GGPP ethers **9**−**11** by five diterpene synthases which are briefly described in the following (Scheme 1B). The diterpene synthase CotB2 catalyzes the cyclization of geranylgeranyl diphosphate (**1**, GGPP) to the tricyclic cyclooctat-9-en-7-ol (**2**), which contains a 5−8−5-fused ring skeleton. It was first found in a strain of the Gram-positive bacterium *Streptomyces melanosporofaciens* MI614-43F2.[18−20] Noteworthy, a fluorinated GGPP derivative was recently employed to mechanistically shed light on the first steps toward cyclooctat-9-en-7-ol (**2**).[21]

Received: January 11, 2025
Revised: March 30, 2025
Accepted: March 31, 2025
Published: April 11, 2025

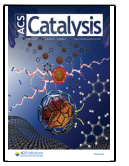

Scheme 1. (A) Natural Cyclization Products 2−6 Formed by the Diterpene Synthases CotB2, PvHVS, PaFS, Bnd4 and TXS (A Detailed Discussion on the Proposed Mechanisms is Found in the Supporting Information); (B) GGPP Derivatives 7 and 8 Recently Employed by Li and Dickschat[16] and GGPP Ether Derivatives 9−11 Studied in This Work (Structural Changes Compared to GGPP 1 Are Marked in Blue)

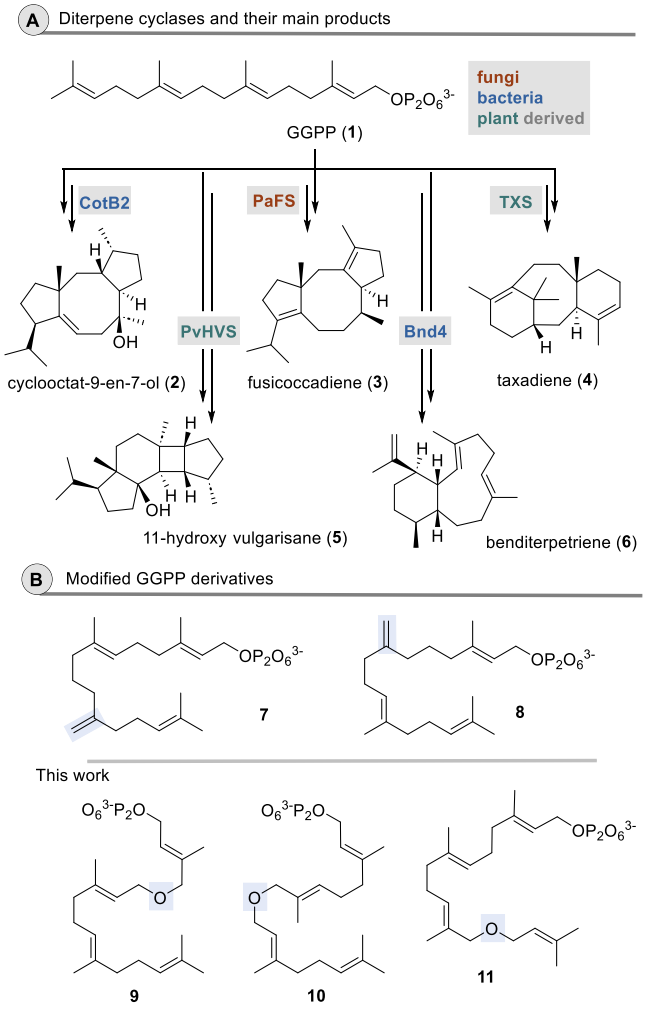

Second, we chose fusicoccadiene synthase (PaFS) isolated from *Phomopsis amygdali* that catalyzes the first two steps in the biosynthesis of the diterpene glycoside fusicoccin A.[22] It is unique in that it is able to catalyze two reactions. First, it acts as a prenyltransferase to form GGPP (**1**) which is then utilized by the enzyme to generate fusicoccadiene (**3**), the tricyclic skeleton of fusicoccin A.[23]

Taxol is a famous diterpene found in the Pacific yew (*Taxus brevifolia*) and the biosynthesis is the cyclization of GGPP **1** to form taxa-4(5),11(12)diene (**4**). This step is catalyzed by taxadiene synthase (TXS).[24] Another diterpene synthase is the vulgarisane synthase (PvHVS), which catalyzes the cyclization of GGPP (**1**) into 11-hydroxy vulgarisane (**5**),[25] the proposed biosynthetic precursor of the vulgarisins.[26] Finally, we selected eunicellane synthase (Bnd4) that is responsible for the formation of the eunicellane diterpenoids. These possess a structurally unique 6,10-bicyclic skeleton with diverse oxidation patterns. Bnd4 transforms GGPP (**1**) into benditerpe-2,6,15-triene (**6**).[27]

RESULTS AND DISCUSSION

Synthesis. First, the three GGPP ether derivatives **9**−**11** had to be prepared starting from prenol (**12**), geraniol (**13**) and farnesol (**14**), respectively (Scheme 2) which were first protected as THP acetals **15**−**17**. After Riley oxidation the resulting alcohols **18**−**20** were transformed into ethers **24**−**26** under Williamson ether synthesis conditions. For that the brominated terpene alcohols **21**−**23** had to be prepared first, again starting from prenol **12**, geraniol **13** and farnesol **14**. After removal of the THP group the resulting alcohols **27**−**29** were transformed into the corresponding diphosphates **9**−**11** according to the two-step protocol reported in detail by Poulter and co-workers.[28]

Biotransformations. For this work the enzymes CotB2, PaFS, PvHVS, Bnd4 and TXS were cloned and expressed in *Escherichia coli* BL21 (DE3). To facilitate protein purification, the plant DTCs PvHVS and TXS were expressed as truncated proteins (see Supporting Information for further details).[26,29] As for PaFS, which is a bifunctional terpene synthase with GGPS and DTC activity, only the DTC domain was expressed.[23,30−32] To determine enzyme activity and substrate tolerance, in vitro assays were performed on a small scale (150 μM, 0.01 g/L) with the natural substrate GGPP **1** as well as the ether derivatives **9**−**11**. Depending on how well the new GGPP ether derivatives were accepted and transformed (as judged by GC−MS; DB-5HT column), semipreparative biotransformations were carried out (1.5 mM, 0.1 g/L) at optimized temperatures to isolate sufficient amounts of biotransformation products which paves the way for structure elucidation. Purification was achieved by normal phase liquid chromatography (NP-HPLC).

A brief overview of the biotransformation results for each enzyme is provided in Table 1. We found that TXS did not transform any of the new GGPP derivatives **9**−**11**. Mechanism-based substrate docking was performed to rationalize the different behavior of TXS by comparing the binding modes of the three substrates with the natural substrate GGPP. The latter adopts a near attack conformation (NAC) suitable for the generation of the first carbocation. The NAC criteria is the C−C distance in the substrate required for cyclization which should be shorter than 4.0 Å.[19]

Through analysis of binding poses of other substrate show that although the three substrates **9**,**10** and **11** had comparable free binding energies (−23 to −25 kcal/mol) to GGPP (−25 kcal/mol) in the top 100 scoring poses out of 1000; however, the required catalytically competent geometry for cyclization and carbocation formation is not fulfilled (Figure 1). Bnd4 did yield new sesquiterpenoids when exposed to GGPP ethers **9** and **10**, but the yields were too low or too many new biotransformation products were detected to practically isolate sufficient quantities of individual products from the mixture suited for structural elucidation. Remarkably, we found that ether derivative **10** was only accepted by $PaFS_{350}$.

Upscaling of the biotransformation of ether derivative **9** with CotB2, provided terpenoid **30**, whose specific structural novelty is associated with the enol ether unit (Scheme 3A).

In addition, diterpene synthase PvHVS yielded tetrahydrofurans **31** and **32** as single diastereomers starting from GGPP derivative **9**. Finally, when GGPP "ethers" **10** and **11** were exposed to the synthase PaFS, the diastereomeric, macrocyclic ether **33** (supposedly two epimeric alcohols) and two prenyl ethers **34** and **35** were found to be formed. The relative stereochemistry of the isolated products was determined by

https://doi.org/10.1021/acscatal.5c00272
ACS Catal. 2025, 15, 6796−6811

Scheme 2. Syntheses of Pyrophosphates 9−11

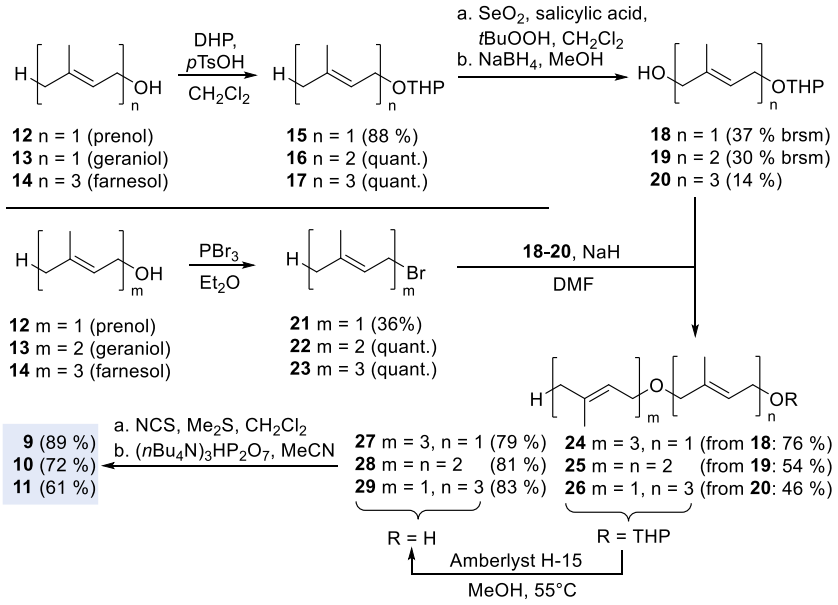

Table 1. Semi-Analytically Expressed Product Formation of the Five Diterpene Synthases with GGPP Derivatives 9−11[a]

GGPP derivative	CotB2	PaFS	TXS	PvHVS	Bnd4
9	+	−	−−	++	−
10	−−	+	−−	−−	−
11	−−	++	−−	−−	+

[a]−−, −, +, ++ they refer to the number and relative quantity of new products judged by GC−MS on which the decision to upscale (see Scheme 3 and Supporting Information) was subsequently based. −− not converted, − converted, + converted, ++ well converted.

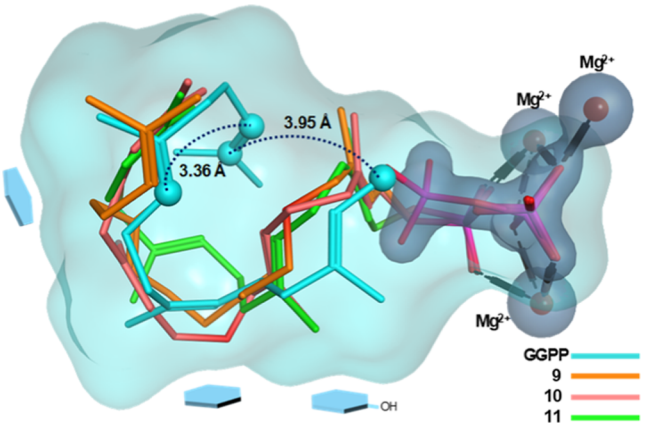

Figure 1. Close-up view of the active site of TXS with the top scoring catalytically competent binding poses of overlaid substrates **9**, **10** and **11** and GGPP. The 3D representation shows the catalytically competent pose of the natural substrate GGPP with the ionic interactions of the pyrophosphate moiety with three Mg^{2+} ions. The conformation (NAC) fulfills the criteria for carbocation formation, stabilization through cation−π interactions with the residues Phe, and Tyr. The overlaid structures of GGPP and substrates **9**, **10** and **11** reveal the difference between the GGPP catalytic binding pose and the noncatalytic highly binding pose of the other substrates. Further details on the docking poses could be found in the Supporting Information (Figures S6 and S7).

NOESY experiments (Scheme 3B). The new terpenoid **30** contains a carbon backbone closely resembling the one of cyclooctat-9-en-7-ol (**2**) so that the 1D and 2D NMR spectra a comparable. However, **30** bears a remarkable cyclic enol ether moiety which was confirmed by the characteristic δ-values for the methine moiety (^{1}H: $\delta_{=CH-O}$ = 6.22 ppm, ^{13}C: $\delta_{-C=CH-O}$ = 110.6 and 139.1 ppm).

Tetrahydrofuran **32** was collected through column chromatography while the nonpolar terpenoid **31** bearing two methylene moieties was isolated by normal phase HPLC. Based on NOE correlations, the configuration of the methyl and CH group in both tetrahydrofuran rings was assigned as *syn*. However, the absolute stereochemistry around the tetrahydrofuran rings for both products as well as the absolute configuration of the tertiary carbinol group in **32** could not be estimated through mechanistic considerations. The structure elucidation of prenyl ethers **34** and **35** (formed in a 3:1 ratio) posed a challenge as the terpenoids could neither be separated by conventional column chromatography nor by normal phase HPLC. In addition to 2D NMR experiments (Scheme 3B), the assignment of the respective constitution also relied on DEPT135 spectra and signal intensities. The structure of the minor product **35** is noteworthy for the presence of the cyclopropane ring, which exhibits the characteristic upfield ^{1}H NMR δ values for the protons [$\delta(CH_2)$ = 0.24, 0.59 ppm, δ(CH) = 0.51 ppm]. The absolute stereochemistry and the underlying cyclization mechanisms reported for the native products were used to propose the absolute stereochemistry of new terpenoids, as outlined below and in Scheme 4.

As the two diastereomeric macroethers **33** (dr = 1:2) could not be separated by column chromatography the structure elucidation by NMR spectroscopy turned out to be a challenge. For NMR characterization, the fraction in which the two diastereomers differed most in their ratio was selected for structural elucidation. It turned out that the sample selected contained the two isomers in inverse ratio to their presence in the isolate (**33a**:**33b** dr = 5:3 by GC analysis and ^{1}H NMR spectroscopically for H12a). The structure elucidation is detailed in the following. 1D and 2D NMR experiments revealed an 11-membered ring as central element and a side

https://doi.org/10.1021/acscatal.5c00272
ACS Catal. 2025, 15, 6796−6811

Scheme 3. (A) Overview of New Diterpenoids 30−35. (B) Key NOE and H2BC[33] NMR Data of New Diterpenoids 30, 34 and 35 for Assignment of the Relative Stereochemistry[a]

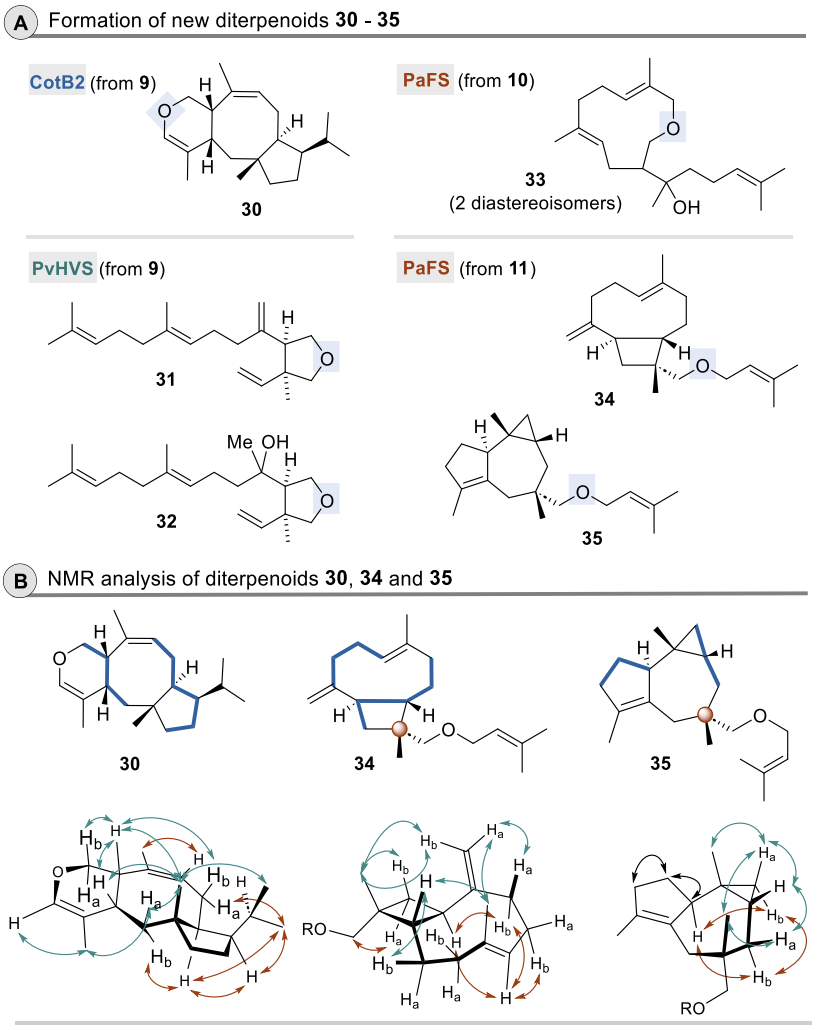

[a]Green arrows = upper side, red arrows = bottom side, black arrows = determination which diastereotopic protons are involved in NOE correlations could not unequivocally be assigned, blue bonds = H2BC correlations. Carbon atoms marked in orange serve as reference point for proposed absolute stereochemistry (structure elucidation of **33** is discussed in the main text).

chain bearing a tertiary alcohol. The $^{1}H-^{13}C$ H2BC NMR experiment (heteronuclear 2-bond correlation)[32] confirmed the connectivity in the ring system. The $^{1}H-^{1}H$ COSY and TOCSY NMR experiments allowed to distinguish the signal sets for the two diastereomers. The major differences of ^{1}H chemical shifts between the two diastereomers are associated with ether methylene groups [especially H12a: $\delta(^{1}H)$ = 3.78 ppm for **33a** and 3.68 ppm for **33b**]. In fact, the signals of H12a, H14a, and H14b are very broadened at ambient temperature (T = 298 K) for both diastereomers. Additionally, we noticed the absence of signals that refer to the CH group (H11 and C11) at 298 K. However, at elevated temperature (T = 333 K) the signals of H12a, H14a, and H14b are well-resolved with a doublet-in-doublet splitting for H12a and H14a as well as a doublet splitting for H14b, respectively. The J-coupling multiplicities excellently fit with the proposed structure. However, due to signal overlap the CH group (H11 and C11) could only be identified by employing selective ^{1}H COSY NMR experiments (SELCOSY). In Figure 2a the ^{1}H NMR spectra (C_6D_6 recorded at 333 K) for isomers **33a** (in blue) and **33b** (in red) are shown. The overlapping signals for both compounds are labeled in purple. Selective ^{1}H COSY NMR experiments employing selective irradiation on the frequency of H12a (cf. Figure 2b,c) reveal signals of adjacent hydrogen atoms. The data confirmed signal assignments for **33a** and **33b** specifically the signals corresponding to H11 at $\delta(^{1}H)$ = 1.55 and 1.53 ppm for **33a** and **33b**. Furthermore, the coupling constants $J_{(HH)}$ = 12.2 and 6.8 Hz for H12a and $J_{(HH)}$ = 12.2 and 1.1 Hz for H12b indicate a pseudoaxial orientation of H11 and consequently the side chain is oriented in a pseudoequatorial orientation. The $^{1}H-^{1}H$ NOESY NMR spectra of **33a** and **33b** recorded at 298 K showed a correlation between the olefinic protons H19 and H14 which were less well resolved at 333 K. Additionally, the two exchange peaks at 2.08/0.40 ppm and 2.85/0.40 ppm refer to the OH groups with the residual water signal (in d6-benzene). The OH signals for the two diastereomers **33a** and **33b** could not be determined due to missing correlations in the $^{1}H-^{1}H$ COSY and $^{1}H-^{13}C$ HMBC NMR spectra. However, the intensities of the cross-correlation signals allowed assignment of $\delta(^{1}H)$ = 2.08 ppm and $\delta(^{1}H)$ = 2.85 ppm for **33b** and **33a**, respectively.

Both carbon skeletons of diterpenoids **34** and **35** can be traced back to the known sesquiterpene skeletons of β-caryophyllene

https://doi.org/10.1021/acscatal.5c00272
ACS Catal. 2025, 15, 6796−6811

Scheme 4. (A) Mechanistic Considerations on the Formation of Diterpene 2; (B) Mechanistic Considerations on the Formation of New Oxaterpenoid 30; (C) Close-Up 3D View of the Active Site of CotB2 with the Catalytic Poses of Intermediate 41−43 and Oxaterpenoid 30[a]

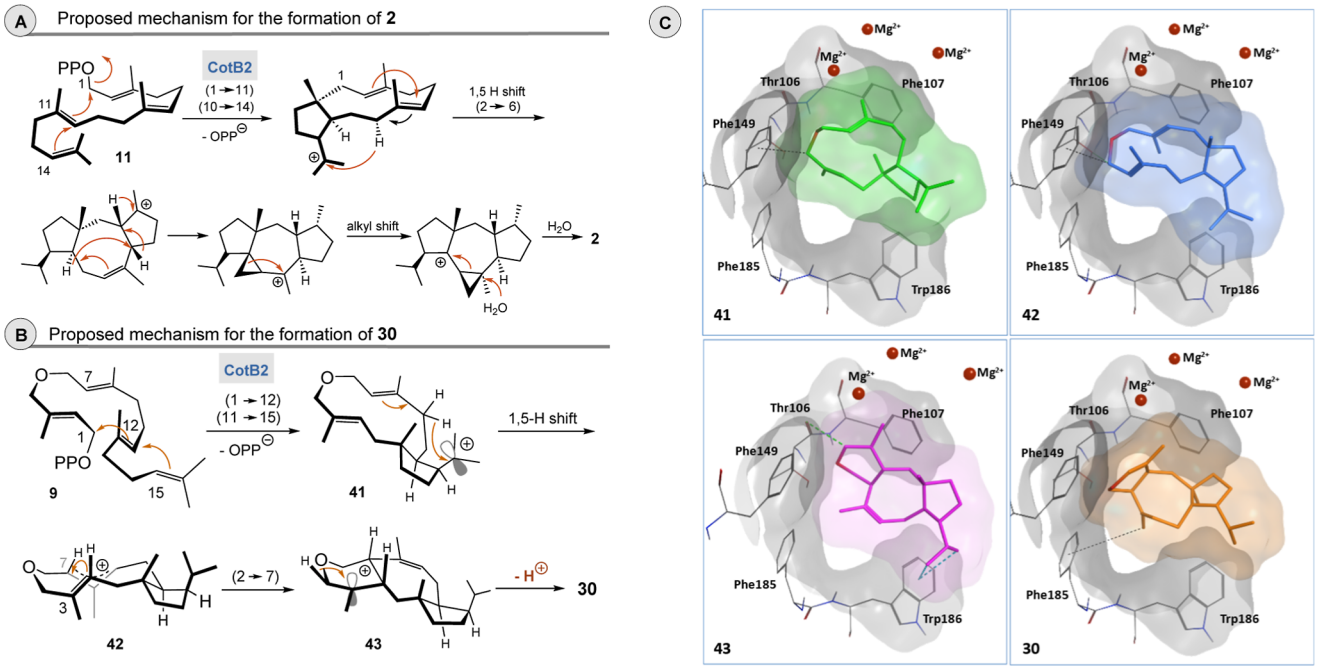

[a]The carbocationic intermediates, proposed in Scheme 4B, are stabilized through cation−π system interactions with the neighboring residues Phe107, Phe149, Phe185, and Trp186 and a key hydrogen bond interaction with Thr106. The additional hydrogen bond interaction of Thr106 with C4−H is shown that promotes deprotonation which is favored over a 1,2-hydride shift and favors the formation of new oxaterpenoid **30**. Detailed 2D representations of the docking poses are found in the Supporting Information (Figures S4 and S5).

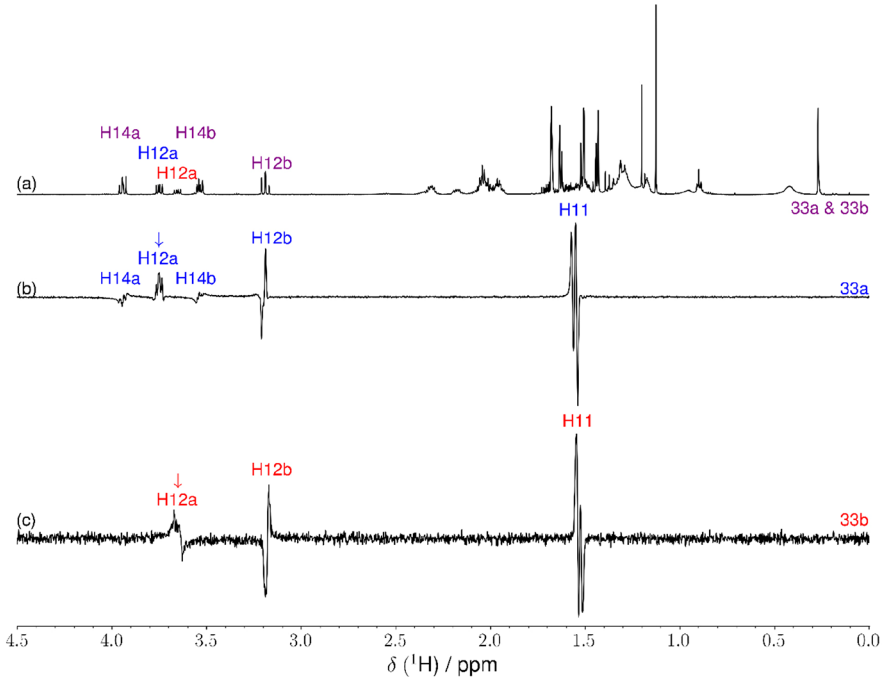

Figure 2. (a) ^{1}H NMR spectra of **33a** and **33b** in C_6D_6 recorded at 14.1 T at 333 K. (b,c) ^{1}H NMR spectra were recorded as selective COSY NMR experiments employing $J_{(HH)}$ = 7 Hz with selective irradiation on H12a at $\delta(^1H)$ = 3.75 and 3.65 ppm, respectively. The blue and red colors indicate the signal assignment to **33a** and **33b**, respectively. Overlapping signals of **33a** and **33b** in the ^{1}H NMR spectrum are highlighted in purple. The selective irradiation frequency is highlighted by the arrow.

(**37**) and african-2-ene (**39**), respectively, except that we have now generated analogs in which one of the two germinal methyl groups is functionalized as a prenyl ether; thus, **34** and **35** are formal stereocontrolled oxidation products of **37** and **39** (Figure 3).[34]

https://doi.org/10.1021/acscatal.5c00272
ACS Catal. 2025, 15, 6796−6811

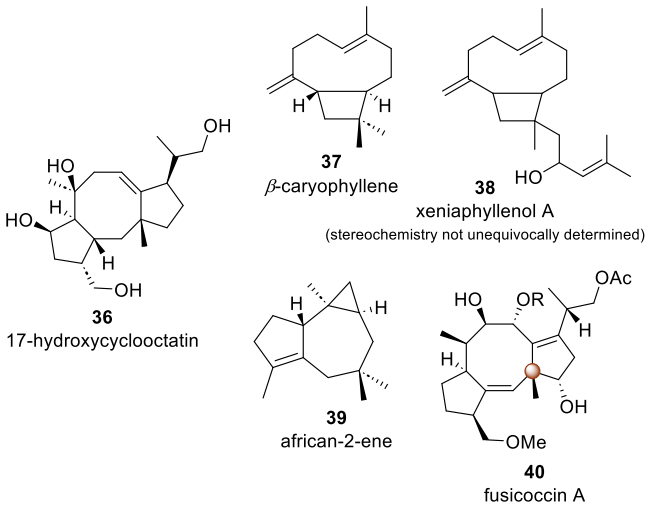

Figure 3. Structures of 17-hydroxycyclooctatin (**36**), β-caryophyllene (**37**), xeniaphyllenol A (**38**), african-2-ene (**39**) and fusicoccin A (**40**) (labeled carbon atom can serve as a reference point for the absolute stereochemistry in terpenoids **34** and **35**).

Mechanistic Considerations. Mechanistically, the formation of cyclooctat-9-en-7-ol (**2**) by CotB2 has been widely debated. According to density functional theory calculations by Hong and Tantillo[35] and consistent with the labeling experiments conducted by Kuzuyama and co-workers[36,37] it is supposed to be initiated by a sequence of 1 → 11 and 10 → 14-cyclizations, followed by a 1,5-hydride shift (Scheme 4A).

This is followed by a series of hydride and alkyl shifts and another cyclization. We suggest that the first part of the sequence also proceeds with the substrate **9** that leads to the formation of enol ether **30**. By analogy, we postulate carbocations **41** and **42**, respectively, as intermediates.

Obviously, the extension of the chain by an additional oxygen atom has no influence on these first steps (**9** → **41** → **42** → **43**) (Scheme 4B). The mechanistic sequence is then terminated by another cyclization that yields the enol ether moiety by deprotonation. Mechanism-based molecular docking of the intermediates for the proposed mechanism A coincides with the reported mechanism of CotB2 for the first steps up to the formation of intermediate **43**. Furthermore, the additional interaction of the oxygen atom and an H-bridge interaction with Thr-106 facilitate deprotonation at C4 rather than a 1,2-hydride shift. During the cascade process, all predicted catalytic poses for the carbocationic intermediates are stabilized through cation−π interactions with the nearby residues Phe107. Phe149, Phe185, Trp186 (Scheme 4C). The absolute configuration was rationalized by comparison of selected stereogenic centers with those found in 17-hydroxycyclooctatin (**36**).[38,39] Its absolute stereochemistry had been secured by a modified version of Mosher's method and the results of this derivatization were taken to propose the absolute stereochemistry of cyclooctat-9-en-7-ol (**2**).

The proposed course of the transformation of GGPP **1** to terpene **5** by PvHVS proceeds via initial (1 → 6 and 2 → 7) cyclizations followed by a series of hydride shifts and another cyclization before the final carbocation is trapped by water (Scheme 5A).

Although the new cyclization products **31** and **32** appear to be structurally quite simple, the question of absolute stereochemistry is not trivial, as one can propose two possible

Scheme 5. (A) Mechanistic Considerations on the Formation of Diterpene 5; (B) Mechanistic Considerations on the Formation New Oxa-Terpenoids 31 and 32

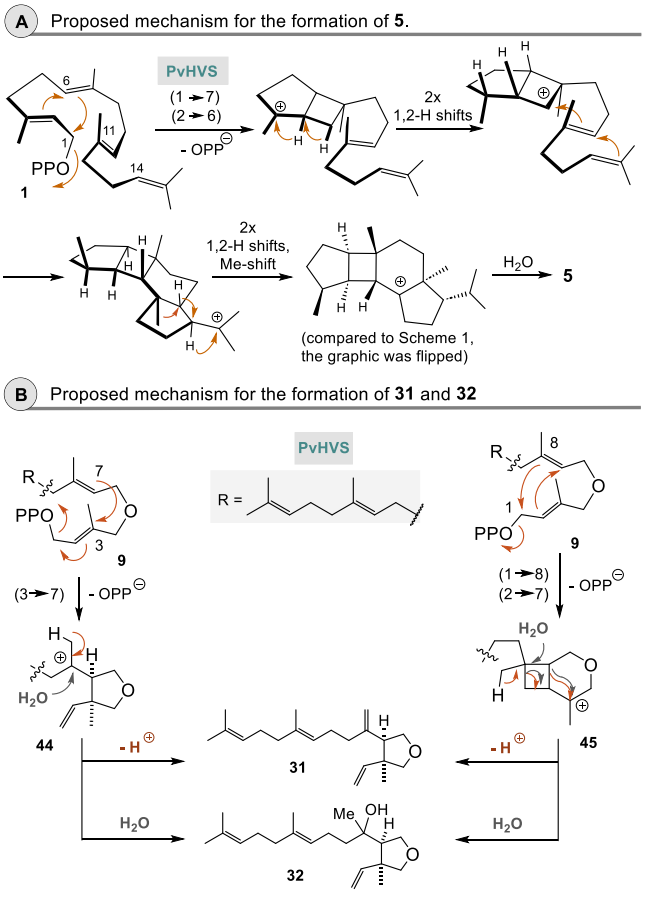

cyclization mechanisms to reach the furan ring starting from the GGPP derivative **10** (Scheme 5b). The simplest route starts with a 3 → 7 cyclization leading to the cation **44**, which is either deprotonated or trapped by water.

On the other hand, analogous to the mechanism proposed for the formation of 11-hydroxy vulgarisane (**5**), successive (1 → 8) and (2 → 7) cyclizations would furnish the cyclobutane intermediate **45**. Next, a Wagner−Meerwein rearrangement would lead to a new ring-opened carbocation that would undergo either deprotonation or water addition to give the tetrahydrofurans **31** and **32**, respectively. Because of this ambiguity or the possibility of alternative routes, the absolute stereochemistry cannot be clearly established by direct comparison with the natural cyclization product of PvHVS, 11-hydroxy vulgarisane (**5**).

In the case of the second route, the stereochemistry shown in Scheme 5B would apply since the methyl group in position 3 corresponds to the single methyl group in the cyclopentane moiety of terpenoid **5**.

The diterpene synthase PaFS transforms GGPP **1** into a bicyclic intermediate via (1 → 11) and (14 → 10) cyclizations (Scheme 6A). This is followed by a series of well-studied hydride, a third cyclization and termination by deprotonation to provide fusicoccadiene **3**.[42] In contrast, the PaFS-mediated formation of diastereomeric, macrocyclic ethers **33** from GGPP derivative **10** is based on a 1 → 11 cyclization followed by trapping of the carbocation by water, that likely occurs from both faces (Scheme 6B). The catalytically competent poses

https://doi.org/10.1021/acscatal.5c00272
ACS Catal. 2025, 15, 6796−6811

Scheme 6. (A) Mechanistic Considerations on the Formation of Diterpene 3; (B,C) Mechanistic Considerations on the Formation New Oxa-Terpenoids 33−35

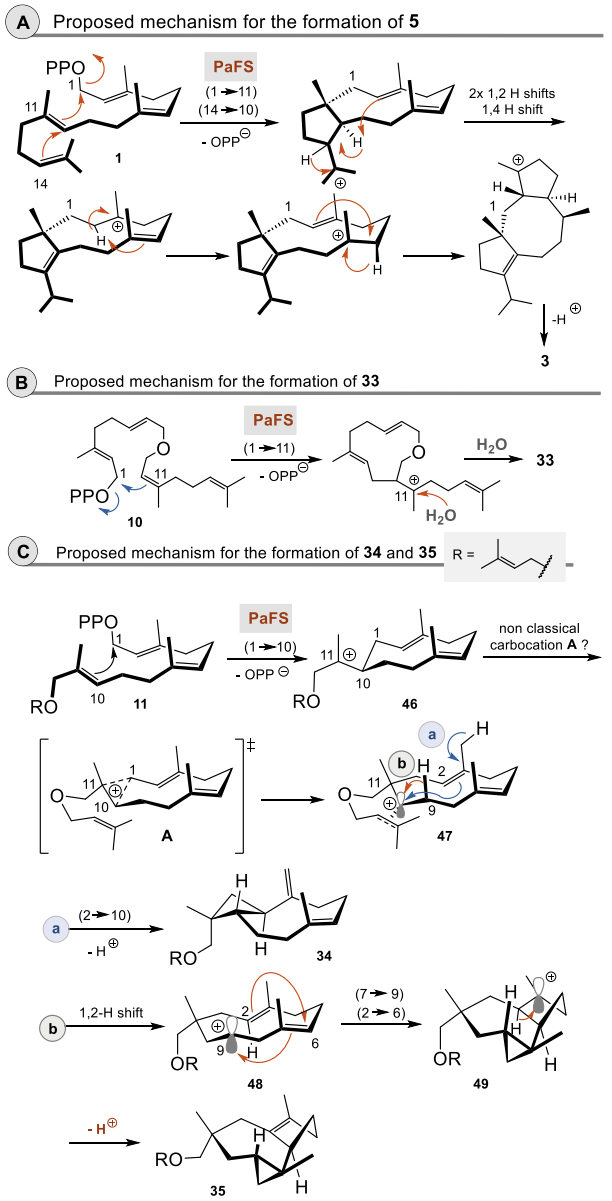

collected from the molecular docking experiments for **10** and **33** are showing strong cation−π system interactions with Phe65 and Phe89 residues which are the key interactions for carbocationic stabilization. Detailed 2D and 3D representations are found in the Supporting Information (Figures S8 and S9).

The formation of the new diterpenoids **34** and **35** from the GGPP derivative **11** by PaFS can be explained by an initial 1 → 11 cyclization to intermediate **46**, and via nonclassical carbocation A to **47**[35,36,41−43] from where subsequent cationic cascades split into two routes **a** and **b** (Scheme 6C). Either a 2 → 10 cyclization followed by deprotonation leads to the caryophyllene derivative **34** (route **a**) or intermediate **47** undergoes a 1,2-hydride shift resulting in the formation of the carbocation **48**. Two cyclizations would follow by which the cyclopropane moiety and the cyclopentane rings are regenerated found in intermediate **49**. The cascade is finally terminated by deprotonation and formation of the olefinic double bond in the african-2-ene derivative **35** (route **b**).

Very recently, Sato et al.[44] carried out a computational analysis on the mechanism that leads to variexenol B from fom *iso*-GGPP **8**, as reported by Dickschat et al.[16] The authors propose that an unstable secondary carbocation (in analogy to **A**) is stabilized by a cation−π interaction induced by the prenyl side chains (R).

This interaction lowers the activation energy, and this might also be a driving force that promotes the transformation of intermediate cation **46** via **A** to **47** (Scheme 6C). The absolute stereochemistry was determined by direct comparison with fusicoccin A (**40**), for which X-ray crystallographic data have been reported.[34] The NOEs between the methyl group at position 11 and both the methyl group and the CH group of the cyclopropane ring indicate a *syn*-orientation. It is expected that the new sesquiterpene analogs **34** and **35** are enantiomeric to their natural relatives **37** and **39**, respectively, when the stereochemistry at C11 is compared with the corresponding position in fusicoccin A (**40**).

Considering that mechanistically only the anterior pyrophosphate moiety of GGPP derivative **9** was involved in the transformation with the sesquiterpene synthase PvHVS, we studied whether the corresponding FPP derivative **50** could serve as a truncated version of **9** in biotransformations with PvHVS. Indeed, when the FPP ether **50**[40] was exposed to PvHVS the corresponding sesquiterpene analogue **51** along with triene byproducts **52** and **53** were isolated (Scheme 7). The relative stereochemistry around the tetrahydrofuran ring was found to be the same as determined for the diterpenoids **31** and **32** (Scheme 5B, bottom).

Scheme 7. Biotransformations of Sesquiterpene Derivative 50 with Diterpene Synthase PvHVS and with PaFS in the Presence of Isopentenyl Pyrophosphate (54) as Well Activity Test for PaFS Using FPP and IPP 54

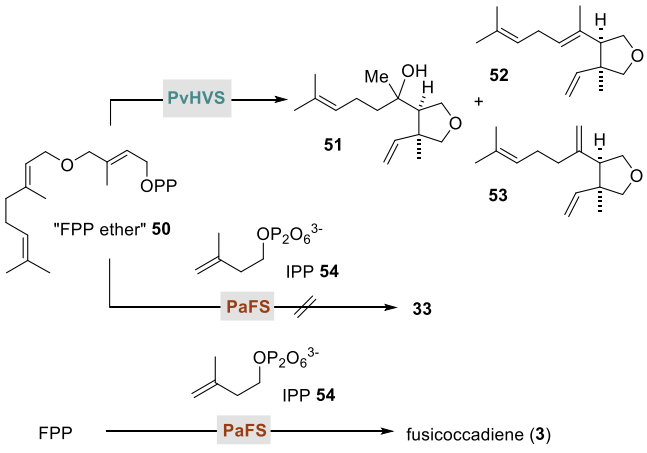

In a second experiment we took FPP derivative **50** and exposed it to the bifunctional full-length terpene synthase PaFS in the presence of in the presence of isopentenyl pyrophosphate (IPP, **54**). A small-scale transformation with $PaFS_{full}$ (scale: 150 μM, 0.01 g/L) revealed no formation of the two expected elongation products **10** or **33**, respectively. However, expectedly farnesyl pyrophosphate was transformed by $PaFS_{full}$ in the presence of IPP **54** into fusicoccadiene (**3**) proving that both enzymatic functions of this unique DTS were active.

https://doi.org/10.1021/acscatal.5c00272
ACS Catal. 2025, 15, 6796−6811

CONCLUSION

In summary, we demonstrated for the first time that GGPP ether derivatives can serve as substrates for DTCs. These results add new examples to the growing body of knowledge that terpene synthases exhibit marked promiscuity toward substrates that are structurally distinct from natural linear pyrophosphate precursors. Compared to STCs, diterpene synthases are less well studied. Therefore, the present results, in addition to those recently published by Dickschat and co-workers,[16,17] rather represent a starting point for further investigations that could ultimately lead to terpene synthases serving as catalytic tools in accessing new terpenoid scaffolds with olfactory or other biological properties.

The results also point to the fact that diterpene synthases accept structurally modified GGPPs less readily than STCs and that the cation cascade then terminates earlier than observed for the native GGPP **1**. This is particularly manifested in the observation that in many cases the terminus of the modified GGPP substrate opposite to the pyrophosphate remains unaltered in the product and thus the shorter FPP derivative **50** behaves like the corresponding GGPP derivative **9**.

METHODS

General Information. ^{1}H NMR spectra were recorded at 400 MHz with a Bruker AVANCE III and Bruker AVANCE IIIHD as well as at 500 MHz with a Bruker AVANCE IIIHD spectrometer or at 600 MHz with a Bruker AVANCE NEO or Bruker Avance III-600 at 298 or 283 K for low temperature NMR measurements. ^{13}C NMR spectra were recorded at 100 MHz with a Bruker AVANCE III and Bruker AVANCE IIIHD or at 125 MHz with a Bruker AVANCE IIIHD or at 151 MHz with a Bruker AVANCE NEO/Avance III-600 instrument. ^{31}P NMR spectra were recorded at 162 MHz with a Bruker AVANCE III. Multiplicities are described using the following abbreviations: s = singlet, d = doublet, t = triplet, q = quartet, qui = quintet, sxt = sextet, spt = septet, m = multiplet, b = broad. Chemical shift values of ^{1}H and ^{13}C NMR spectra are commonly reported in ppm relative to residual solvent signal as internal standard $\delta(CDCl_3) = 7.26$ ppm, $\delta(C_6D_6) = 7.16$ ppm, $\delta(D_2O) = 4.79$ ppm and $\delta(CD_3OD) = 3.31$ ppm for ^{1}H, $\delta(CDCl_3) = 77.16$ ppm, $\delta(C_6D_6) = 128.06$ ppm and $\delta(CD_3OD) = 49.00$ ppm for ^{13}C]. The multiplicities refer to the resonances in the off-resonance decoupled spectra and were elucidated using phase-sensitive HSQC experiments. Mass spectra were obtained with a lockspray dual ion source in combination with a WATERS Alliance 2695 LC system, or with a type Q-TOF premier (MICROMASS) spectrometer (ESI mode) in combination with a WATERS Acquity UPLC system equipped with a WATERS Acquity UPLC BEH C18 1.7 μm (SN 01473711315545) column (solvent A: water +0.1% {v/v} formic acid, solvent B: MeCN or MeOH {given in experimental part} + 0.1% {v/v} formic acid; flow rate = 0.4 mL/min; gradient {t [min]/solvent B [%]}: {0/5} {2.5/95} {6.5/95} {6.6/5} {8/5}; retention times {r_t} given in the experimental part). Ion mass signals (m/z) are reported as values in atomic mass units.

GC/MS analyzes were carried out on with an Agilent 7890B GC with 5977B GC/MSD and Gerstel MPS Robotic XL with KAS 4C injector. Samples were analyzed on an Optima 5HT column (30 m × 250 μm i.d. × film thickness 0.25 μm). Carrier gas, He; injector temp.: 60−300 °C at 12 °C/min, splitless or split ratio 1:40; temp. program: 50 °C (isothermal 1 min) to 300 °C, at 20 °C/min and held isothermal for 6.5 min at 300 °C; FID: 300 °C, H_2: 30 mL/min, N_2: 25 mL/min, MSD: ion source: EI 70 eV, 230 °C; detector: quadrupole, EI mass spectra were acquired over the mass range of 30−650 amu. Further GC/MS analyzes were carried out with an Agilent GC 7890B chromatograph with Gerstel CIS4 Cold Injector. Samples were analyzed on an Optima WAX column (30 m × 0.25 mm i.d. × film thickness 0.25 μm). Carrier gas, He; injector temp.: 50−250 °C at 12 °C/min; split ratio 1:40; temp. program: 60 °C (isothermal 1 min) to 240 °C at 9 °C/s held isothermal for 9 min at 240 °C; FID: 250 °C, H_2: 40 mL/min, N_2: 45 mL/min, MSD: ion source: EI 70 eV, 230 °C; detector: quadrupole.

HR-GC/MS analyzes were carried out on a Waters GCT Premier mass spectrometer coupled with an Agilent 6890n GC with CTC CombiPAL sampler. Samples were analyzed on an Optima 5HT column (30 m × 250 μm i.d. × film thickness 0.25 μm). Carrier gas, He; injector temp. 300 °C, split ratio 1:40; temp. program: 50 °C (isothermal 1 min) to 300 °C, at 20 °C/min and held isothermal for 6.5 min at 300 °C; FID: 300 °C, H_2: 30 mL/min, N_2: 25 mL/min, GCT-Premier: ion source: EI 70 eV, 250 °C; detector-voltage: 2500 V, EI mass spectra were acquired over the mass range of 20−800 amu.

SP-NP-HPLC: Purification with semipreparative HPLC were carried out with L-7100 and L-7170 pump, D 7000 interface and L-7455 diode array detector (λ = 200−350 nm) by MERCK HITACHI and a VP 250/10 Nucleodur 100−5 CN-RP column (5 μm, 250 mm, Ø 10 mm) by MACHEREY-NAGEL.

P-NP-HPLC: Purification with preparative HPLC were carried out GILSON HPLC-system (pump 331/332) with additional MERCK HITACHI Split-Pump (L-6200A, UV−vis detector L-4250) and a chiral PHENOMENEX Lux Cellulose-1 preparative column (5 μm, 250, Ø 21.2 mm).

Preparative GC (pGC) with a ZB-1 column (Phenomenex, 30 m × 0.53 mm i.d. × 3 μm film thickness, serial no. 628795) or a ZB-WAX*plus* column (Phenomenex, 30 m × 0.53 mm i.d. × 3 μm film thickness, serial no. 1095497) was carried out on a HP 6890 chromatograph with HP 7683 autosampler and hot injection. New terpenoids were isolated with a Gerstel PFC. The temperature gradient was optimized for each isolation, carrier gas: H_2 (5 mL/min), injector temp.: 250 °C, splitless, injection volume: 1 μL, detector: FID, temperature: 250 °C, H_2: 40 mL/min, N_2: 45 mL/min.

Analytical thin-layer chromatography (TLC) was performed using precoated silica gel plates (Macherey-Nagel, Düren) and the spots were visualized by staining with anisaldehyde or vanillin solutions.[26] Commercially available reagents, chromatography type or dry solvents were used as received or purified by standard techniques according to the literature.[44]

Chemical Synthesis. *General Procedure for THP Protection (Products **15**−**17**).* The alcohol (1.0 equiv) was dissolved in CH_2Cl_2 (0.3 M) and pTsOH·H_2O (0.02 equiv) as added at 0 °C. Then, DHP (2.0 equiv) was slowly added at 0 °C and the reaction mixture was stirred at 0 °C for 2 h. The reaction was terminated by adding a semisaturated solution of $NaHCO_3$. The phases were separated and the aqueous phase was extracted with CH_2Cl_2 (3×). The combined organic phases were dried and the solvent was removed under reduced pressure.

*2-((3-Methylbut-2-en-1-yl)oxy)tetrahydro-2H-pyran (**15**).* After THP protection of prenol (**12**, 600 mg, 0.71 mL, 6.97 mmol), the crude product was purified by column chromatography (PE/EtOAc = 5:1) to give volatile product **15** (1.04 g, 6.11 mmol, 88%) as a colorless oil.

^{1}H NMR (400 MHz, $CDCl_3$): δ (ppm) = 5.39−5.33 (m, 1H, H-3), 4.62 (dd, J = 4.5, 2.9 Hz, 1H, H-6), 4.22 (dd, J = 11.7, 6.6

https://doi.org/10.1021/acscatal.5c00272
ACS Catal. 2025, 15, 6796−6811

Hz, 1H, H_a-4), 3.99 (dd, J = 11.7, 7.6 Hz, 1H, H_b-4), 3.92−3.86 (m, 1H, H_a-10), 3.54−3.48 (m, 1H, H_b-10), 1.90−1.47 (m, 6H, H-7/8/9), 1.75 (s, 3H, H-5), 1.68 (s, 3H, H-1); **^{13}C NMR** (100 MHz, $CDCl_3$): δ (ppm) = 137.2 (C-2), 121.0 (C-3), 98.0 (C-6), 63.8 (C-4), 62.4 (C-10), 30.8 (C-7/8/9), 26.0 (C-7/8/9), 25.6 (C-1), 19.8 (C-7/8/9), 18.1 (C-5).

*(E)-2-((3,7-Dimethylocta-2,6-dien-1-yl)oxy)tetrahydro-2H-pyran (**16**).* After THP protection of geraniol (**13**, 1.00 g, 1.14 mL, 6.48 mmol), the crude product was purified by column chromatography (PE/EtOAc = 5:1) to give product **16** (1.55 g, 6.48 mmol, quant.) as a colorless oil.

^{1}H NMR (400 MHz, $CDCl_3$): δ (ppm) = 5.38−5.33 (m, 1H, H-7), 5.12−5.07 (m, 1H, H-3), 4.62 (dd, J = 4.5, 2.9 Hz, 1H, H-11), 4.23 (ddsxt, J = 11.9, 6.4, 0.8 Hz, 1H, H_a-8), 4.03 (ddsxt, J = 11.9, 7.4, 0.6 Hz, 1H, H_b-8), 3.92−3.87 (m, 1H, H_a-15), 3.54−3.48 (m, 1H, H_b-15), 2.14−2.08 (m, 2H, H-4/5), 2.06−2.01 (m, 2H, H-4/5), 1.89−1.47 (m, 6H, H-12/13/14), 1.68 (s, 3H, H-1), 1.67 (s, 3H, H-10), 1.60 (s, 3H, H-9); **^{13}C NMR** (100 MHz, $CDCl_3$): δ (ppm) = 140.4 (C-6), 131.8 (C-2), 124.2 (C-3), 120.7 (C-7), 97.9 (C-11), 63.8 (C-8), 62.4 (C-15), 39.8 (C-5), 30.9 (C-12/13/14), 26.5 (C-4), 25.8 (C-12/13/14), 25.7 (C-1), 19.8 (C-12/13/14), 17.8 (C-9), 16.5 (C-10).

*2-(((2E,6E)-3,7,11-Trimethyldodeca-2,6,10-trien-1-yl)oxy)-tetrahydro-2H-pyran (**17**).* After THP protection of farnesol (**14**, 2.50 g, 2.82 mL, 11.24 mmol), the crude product was purified by column chromatography (PE/EtOAc = 8:1) to give product **17** (3.45 g, 11.24 mmol, quant.) as a colorless oil.

^{1}H NMR (400 MHz, $CDCl_3$): δ (ppm) = 5.38−5.34 (m, 1H, H-11), 5.13−5.08 (m, 1H, H-7), 5.11−5.06 (m, 1H, H-3), 4.62 (dd, J = 4.5, 2.9 Hz, 1H, H-16), 4.24 (ddsxt, J = 11.9, 6.4, 0.7 Hz, 1H, H_a-12), 4.03 (dd, J = 11.9, 7.4 Hz, 1H, H_b-12), 3.92−3.87 (m, 1H, H_a-20), 3.54−3.48 (m, 1H, H_b-20), 2.15−2.09 (m, 2H, H-8), 2.07−2.03 (m, 4H, H-4/9), 1.99−1.95 (m, 2H, H-5), 1.91−1.48 (m, 6H, H-17/18/19), 1.68 (s, 6H, H-1/15), 1.60 (s, 6H, H-13/14); **^{13}C NMR** (100 MHz, $CDCl_3$): δ (ppm) = 140.4 (C-10), 135.4 (C-6), 131.5 (C-2), 124.5 (C-3), 124.0 (C-7), 120.7 (C-11), 97.9 (C-16), 63.8 (C-12), 62.4 (C-20), 39.9 (C-5), 39.8 (C-9), 30.9 (C-17/18/19), 26.9 (C-4), 26.4 (C-8), 25.8 (C-1), 25.7 (C-17/18/19), 19.8 (C-17/18/19), 17.8 (C-13), 16.6 (C-15), 16.2 (C-14).

*General Procedure for Riley Oxidation (Products **18**−**20**).* SeO_2 (0.1 equiv) and salicylic acid (0.1 equiv) were dissolved in CH_2Cl_2 (0.25 M) at rt. After addition of tBuOOH (70% in H_2O, 3.5 equiv), the reaction mixture was stirred at rt for 10 min. The THP-protected alcohol (1.0 equiv) was added, followed by vigorous stirring at rt for 2 days. The reaction was terminated by the addition of a semisaturated $NaHCO_3$ solution and the phases were separated. The aqueous phase was extracted with MTBE (3×). The combined organic phases were dried and concentrated under reduced pressure. The resulting oil was dissolved in MeOH (0.25 M) and $NaBH_4$ (1.0 equiv) was added portionwise at 0 °C. When the reaction was completed after 20 min as judged by TLC, it was terminated by slow addition of a semisaturated NH_4Cl solution and dilution with MTBE. After phase separation the aqueous phase was extracted three times with MTBE. The combined organic phases were dried and the solvent was removed under reduced pressure.

*(E)-2-Methyl-4-((tetrahydro-2H-pyran-2-yl)oxy)but-2-en-1-ol (**18**).* After oxidation of THP-protected prenol **15** (500 mg, 2.94 mmol), the crude product was purified by column chromatography (PE/EtOAc = 5:1) to give the desired alcohol **18** (166 mg, 0.891 mmol, 37% brsm) as a pale-yellow oil.

^{1}H NMR (400 MHz, C_6D_6): δ (ppm) = 5.73−5.68 (m, 1H, H-3), 4.68 (t, J = 3.4 Hz, 1H, H-6), 4.37 (ddsxt, J = 12.1, 6.3, 0.9 Hz, 1H, H_a-4), 4.07 (ddsxt, J = 12.1, 7.1, 0.7 Hz, 1H, H_b-4), 3.70 (s, 2H, H-1), 3.87−3.81 (m, 1H, H_a-10), 3.44−3.39 (m, 1H, H_b-10), 1.86−1.56 (m, 3H, H-7/8/9), 1.71 (m, 3H, H-5), 1.44−1.22 (m, 3H, H-7/8/9); **^{13}C NMR** (100 MHz, C_6D_6): δ (ppm) = 138.8 (C-2), 121.8 (C-3), 97.7 (C-6), 67.9 (C-1), 63.4 (C-4), 61.6 (C-10), 31.1 (C-7/8/9), 26.0 (C-7/8/9), 19.6 (C-7/8/9), 13.7 (C-5).

*(2E,6E)-2,6-Dimethyl-8-((tetrahydro-2H-pyran-2-yl)oxy)-octa-2,6-dien-1-ol (**19**).* After oxidation of THP-protected geraniol **16** (550 mg, 2.31 mmol), the crude product was purified by column chromatography (PE/EtOAc = 4.5:1−3:1) to give the desired alcohol **19** (154 mg, 0.607 mmol, 30% brsm) as a pale-yellow oil.

^{1}H NMR (400 MHz, C_6D_6): δ (ppm) = 5.56−5.52 (m, 1H, H-3), 5.33−5.28 (tsxt, J = 7.2, 1.3 Hz, 1H, H-7) 4.70 (t, J = 3.4 Hz, 1H, H-11), 4.38 (dd, J = 12.0, 6.4 Hz, 1H, H_a-8), 4.07 (dd, J = 12.0, 7.2 Hz, 1H, H_b-8), 3.88−3.82 (m, 1H, H_a-15), 3.80 (s, 2H, H-1), 3.45−3.39 (m, 1H, H_b-15), 2.11−2.06 (m, 2H, H-4), 2.02−1.98 (m, 2H, H-5), 1.85−1.58 (m, 3H, H-12/13/14), 1.57 (s, 3H, H-9), 1.53 (s, 3H, H-10), 1.44−1.22 (m, 3H, H-12/13/14); **^{13}C NMR** (100 MHz, C_6D_6): δ (ppm) = 139.0 (C-2), 135.9 (C-6), 125.0 (C-7), 122.3 (C-3), 97.6 (C-11), 68.8 (C-1), 63.7 (C-8), 61.6 (C-15), 39.5 (C-5), 31.1 (C-12/13/14), 26.1 (C-12/13/14), 26.0 (C-4), 19.6 (C-12/13/14), 16.3 (C-9), 13.7 (C-10).

*(2E,6E,10E)-2,6,10-Trimethyl-12-((tetrahydro-2H-pyran-2-yl)oxy)dodeca-2,6,10-trien-1-ol (**20**).* After oxidation of THP-protected farnesol **17** (3.56 g, 11.24 mmol), the crude product was purified by column chromatography (PE/EtOAc = 4.5:1−2:1) to give the desired alcohol **20** (511 mg, 1.58 mmol, 14%) as a pale-yellow oil.

^{1}H NMR (400 MHz, C_6D_6): δ (ppm) = 5.61−5.57 (m, 1H, H-3), 5.42−5.37 (tsxt, J = 7.2, 1.3 Hz, 1H, H-11), 5.23−5.19 (m, 1H, H-7) 4.72 (t, J = 3.4 Hz, 1H, H-16), 4.40 (dddd, J = 12.0, 6.3, 0.8, 0.6 Hz, 1H, H_a-12), 4.14 (dd, J = 12.0, 7.3 Hz, 1H, H_b-12), 3.89−3.82 (m, 1H, H_a-20), 3.83 (s, 2H, H-1), 3.45−3.40 (m, 1H, H_b-20), 2.17−2.11 (m, 4H, H-4/-8), 2.06−2.03 (m, 4H, H-5/-9), 1.85−1.61 (m, 2H, H-17/18/19), 1.60 (s, 3H, H-13), 1.57 (s, 3H, H-14), 1.55 (s, 3H, H-15), 1.44−1.23 (m, 4H, H-17/18/19); **^{13}C NMR** (100 MHz, C_6D_6): δ (ppm) = 139.1 (C-2), 135.5 (C-10), 134.9 (C-6), 125.1 (C-11), 124.7 (C-7), 122.2 (C-3), 97.4 (C-16), 68.7 (C-1), 63.7 (C-12), 61.6 (C-20), 39.9 (C-9), 39.8 (C-5), 31.1 (C-17/18/19), 26.6 (C-8), 26.4 (C-4), 26.0 (C-17/18/19), 19.6 (C-17/18/19), 16.4 (C-13), 16.1 (C-14), 13.7 (C-15).

*General Procedure for the Bromination of Linear Terpene Alcohols (Products **21**−**23**).* The corresponding terpene alcohol (1.0 equiv) was dissolved in dry Et_2O (0.18 M) at 0 °C, PBr_3 (0.5 equiv) was slowly added and the reaction mixture was stirred at 0 °C. The complete conversion was monitored by TLC. After the addition of a saturated $NaHCO_3$ solution at 0 °C, the reaction was diluted with Et_2O and brine. After phase separation, the organic phase was washed three times with brine, dried and concentrated under reduced pressure.

*1-Bromo-3-methylbut-2-ene (**21**).* After bromination of prenol (**12**, 310 mg, 0.37 mL, 3.60 mmol), the resulting volatile bromide **21** (192 mg, 1.30 mmol, 36%) was used directly in the next synthesis step without further purification.

^{1}H NMR (400 MHz, $CDCl_3$): δ (ppm) = 5.52 (t, J = 8.5 Hz, 1H, H-3), 4.01 (d, J = 8.5 Hz, 2H, H-4), 1.78 (s, 3H, H-5), 1.73 (s, 3H, H-1).

https://doi.org/10.1021/acscatal.5c00272
ACS Catal. 2025, 15, 6796−6811

*(E)-1-Bromo-3,7-dimethylocta-2,6-diene (**22**).* After bromination of geraniol (**13**, 1.11 g, 1.26 mL, 7.16 mmol), the resulting bromide **22** (1.55 g, 7.16 mmol, quant.) was used directly in the next synthesis step without further purification.

^{1}H NMR (400 MHz, $CDCl_3$): δ (ppm) = 5.53 (t, J = 8.4 Hz, 1H, H-7), 5.09−5.05 (m, 1H, H-3), 4.03 (d, J = 8.4 Hz, 2H, H-8), 2.14−2.04 (m, 4H, H-4/5) 1.73 (s, 3H, H-9), 1.68 (s, 3H, H-1), 1.60 (s, 3H, H-10).

*(2E,6E)-1-Bromo-3,7,11-trimethyldodeca-2,6,10-triene (**23**).* After bromination of farnesol (**14**, 574 mg, 0.65 mL, 2.58 mmol), the resulting bromide **23** (736 mg, 2.58 mmol, quant.) was used directly in the next synthesis step without further purification.

^{1}H NMR (400 MHz, $CDCl_3$): δ (ppm) = 5.53 (tsxt, J = 8.4, 1.3 Hz, 1H, H-11), 5.11−5.06 (m, 2H, H-3/7), 4.02 (d, J = 8.4 Hz, 2H, H-12), 2.15−2.04 (m, 6H, H-4/5/9), 2.01−1.96 (m, 2H, H-8) 1.73 (d, J = 1.3 Hz, 3H, H-13), 1.68 (m, 3H, H-1), 1.60 (br s, 6H, H-14/15).

*General Procedure for the Williamson Ether Synthesis (Products **24**−**26**).* To a freshly prepared suspension of NaH (90% in mineral oil, 1.5 equiv) in DMF (0.55 M), the alcohol (1.0 equiv) in DMF (1.8 M) was added dropwise at 0 °C and stirred for 45 min at rt. Then, the corresponding bromide (1.0 equiv) was added slowly at 0 °C and the reaction mixture was stirred for 18 h at RT. The reaction was terminated by the addition of a semisaturated NH_4Cl solution. The aqueous phase was extracted with EtOAc (3×) and the combined organic phases were then washed twice with water and brine, dried and concentrated under reduced pressure.

*2-(((E)-3-Methyl-4-(((2E,6E)-3,7,11-trimethyldodeca-2,6,10-trien-1-yl)oxy)but-2-en-1-yl)oxy)-tetrahydro-2H-pyran (**24**).* Williamson ether synthesis using alcohol **18** (1.20 g, 6.44 mmol) and farnesyl bromide **23** (1.84 g, 6.44 mmol) as starting materials gave the desired ether **24** (1.86 g, 4.76 mmol, 76%) as a yellow oil after column chromatography (PE/EtOAc = 10:1).

R_f (PE/EtOAc = 1:1): 0.65; **^{1}H NMR** (400 MHz, $CDCl_3$): δ (ppm) = 5.64−5.60 (m, 1H, H-15), 5.38−5.34 (m, 1H, H-11), 5.13−5.06 (m, 2H, H-7/3), 4.63 (dd, J = 4.1, 3.0 Hz, 1H, H-21), 4.29 (ddq, J = 12.3, 6.3, 0.8 Hz, 1H, H_a-16), 4.08 (ddq, J = 12.3, 7.2, 0.6 Hz, 1H, H_b-16), 3.94 (d, J = 6.8 Hz, 2H, H-12), 3.91−3.86 (m, 1H, H_a-25), 3.54−3.49 (m, 1H, H_b-25), 3.87 (s, 2H, H-13), 2.14−2.09 (m, 2H, H-8), 2.07−2.02 (m, 4H, H-4/9), 1.99−1.95 (m, 2H, H-5), 1.71 (br s, 3H, H-20), 1.68 (m, 3H, H-19), 1.66 (br s, 3H, H-1), 1.60 (br s, 6H, H-17/18); **^{13}C NMR** (100 MHz, $CDCl_3$): δ (ppm) = 140.3 (C-10), 136.7 (C-14), 135.4 (C-6), 131.5 (C-2), 124.5 (C-3), 124.0 (C-7), 123.8 (C-15), 121.0 (C-11), 98.1 (C-21), 75.5 (C-13), 66.4 (C-12), 63.4 (C-16), 62.4 (C-25), 39.9 (C-5), 39.8 (C-9), 30.8 (C-22/23/24), 26.9 (C-4), 26.5 (C-8), 25.8 (C-1), 25.6 (C-22/23/24), 19.7 (C-22/23/24), 17.8 (C-17), 16.6 (C-19), 16.2 (C-18), 14.3 (C-20); **HRMS** (ESI) m/z calcd for $C_{25}H_{42}O_3Na^+$ $[M + Na]^+$, 413.3032; found, 413.3037.

*2-(((2E,6E)-8-(((E)-3,7-Dimethylocta-2,6-dien-1-yl)oxy)-3,7-dimethylocta-2,6-dien-1-yl)oxy)tetra-hydro-2H-pyran (**25**).* Williamson ether synthesis using alcohol **19** (1.40 g, 5.51 mmol) and geranyl bromide **22** (1.20 g, 5.51 mmol) as starting materials gave the desired ether **25** (1.15 g, 2.95 mmol, 54%) as a yellow oil after column chromatography (PE/EtOAc = 10:1).

R_f (PE/EtOAc = 1:1): 0.68; **^{1}H NMR** (400 MHz, $CDCl_3$): δ (ppm) = **^{1}H NMR** (400 MHz, $CDCl_3$): δ (ppm) = 5.41−5.33 (m, 3H, H-11/15/7), 5.12−5.07 (m, 1H, H-3), 4.62 (dd, J = 4.2, 2.9 Hz, 1H, H-21) 4.24 (ddq, J = 11.9, 6.4, 0.7 Hz, 1H, H_a-16), 4.02 (dd, J = 11.9, 7.3 Hz, 1H, H_b-16), 3.93−3.86 (m, 1H, H_a-25), 3.91 (d, J = 6.7 Hz, 2H, H-8), 3.83 (s, 2H, H-9) 3.54−3.48 (m, 1H, H_b-25), 2.21−2.14 (m, 2H, H-12), 2.12−2.06 (m, 4H, H-4/13), 2.05−2.01 (m, 2H, H-5), 1.88−1.50 (m, 6H, H-22/23/24) 1.68 (br s, 6H, H-20/1), 1.65 (br s, 6H, H-19/18), 1.60 (br s, 3H, H-17); **^{13}C NMR** (100 MHz, $CDCl_3$): δ (ppm) = 140.1 (C-10), 140.0 (C-6), 132.8 (C-14), 131.8 (C-2), 127.7 (C-11), 124.2 (C-3), 121.2 (C-7), 120.9 (C-15), 98.0 (C-21), 76.2 (C-9), 66.0 (C-8), 63.8 (C-16), 62.4 (C-25), 39.8 (C-5), 39.4 (C-13), 30.9 (C-22/23/24), 26.5 (C-4), 26.2 (C-12), 25.8 (C-1), 25.7 (C-22/23/24), 19.8 (C-22/23/24), 17.8 (C-17), 16.6 (C-18), 16.5 (C-20), 14.1 (C-19); **HRMS** (ESI) m/z calcd for $C_{25}H_{42}O_3Na^+$ $[M + Na]^+$, 413.3032; found, 413.3019.

*2-(((2E,6E,10E)-3,7,11-Trimethyl-12-((3-methylbut-2-en-1-yl)oxy)dodeca-2,6,10-trien-1-yl)oxy)tetrahydro-2H-pyran (**26**).* Williamson ether synthesis using alcohol **20** (880 mg, 2.73 mmol) and prenyl bromide **21** (404 mg, 2.73 mmol) as starting materials gave the desired ether **26** (489 mg, 1.25 mmol, 46%) as a yellow oil after column chromatography (PE/EtOAc = 10:1).

R_f (PE/EtOAc = 1:1): 0.58; **^{1}H NMR** (400 MHz, $CDCl_3$): δ (ppm) = 5.41−5.33 (m, 3H, H-11/15/7), 5.12 (tq, J = 6.9, 1.2 Hz, 1H, H-3), 4.62 (dd, J = 4.5, 2.8 Hz, 1H, H-21) 4.24 (dd, J = 11.9, 6.4 Hz, 1H, H_a-16), 4.02 (dd, J = 11.9, 7.4 Hz, 1H, H_b-16), 3.92−3.86 (m, 1H, H_a-25), 3.91 (d, J = 6.8 Hz, 2H, H-8), 3.83 (s, 2H, H-9) 3.54−3.48 (m, 1H, H_b-25), 2.16−2.08 (m, 2H, H-12), 2.06−1.99 (m, 4H, H-4/13), 2.05−2.01 (m, 2H, H-5), 1.88−1.50 (m, 6H, H-22/23/24) 1.68 (br s, 6H, H-20/1), 1.65 (br s, 6H, H-19/18), 1.60 (br s, 3H, H-17); **^{13}C NMR** (100 MHz, $CDCl_3$): δ (ppm) = 140.4 (C-10), 136.8 (C-6), 135.1 (C-14), 132.5 (C-2), 128.1 (C-11), 124.3 (C-3), 121.5 (C-7), 120.8 (C-15), 98.0 (C-21), 76.4 (C-9), 65.9 (C-8), 63.8 (C-16), 62.4 (C-25), 39.8 (C-5), 39.5 (C-13), 30.9 (C-22/23/24), 26.5 (C-4), 26.4 (C-12), 25.9 (C-1), 25.7 (C-22/23/24), 19.8 (C-22/23/24), 18.2 (C-17), 16.6 (C-18), 16.1 (C-20), 14.1 (C-19); **HRMS** (ESI) m/z calcd for $C_{25}H_{42}O_3Na^+$ $[M + Na]^+$, 413.3032; found, 413.3045.

*General Procedure for THP Deprotection (Products **27**−**29**).* The compound to be deprotected (1.0 equiv) was dissolved in MeOH (0.5 M) and Amberlyst H-15 (0.1 equiv) was added. The reaction mixture was stirred at 50 °C for 1.5 h and the end of the reaction was determined by TLC. After filtering off the polymer and rinsing with CH_2Cl_2, the organic phases were concentrated under reduced pressure.

*(E)-3-Methyl-4-(((2E,6E)-3,7,11-trimethyldodeca-2,6,10-trien-1-yl)oxy)but-2-en-1-ol (**27**).* After deprotection of compound **24** (390 mg, 1.00 mmol), ether **27** (242 mg, 0.790 mmol, 79%) was obtained as a light-yellow oil after column chromatography (PE/EtOAc = 5:1 → 4.5:1).

R_f (PE/EtOAc = 1:1): 0.40; **^{1}H NMR** (400 MHz, $CDCl_3$): δ (ppm) = 5.66 (tsxt, J = 6.8, 1.4 Hz, 1H, H-15), 5.35 (tsxt, J = 6.8, 1.3 Hz, 1H, H-11), 5.13−5.07 (m, 2H, H-7/3), 4.21 (dsxt, J = 6.8, 0.7 Hz, 2H, H-16), 3.95 (d, J = 6.8 Hz, 2H, H-12), 3.86 (s, 2H, H-13), 2.14−2.09 (m, 2H, H-5), 2.07−2.02 (m, 4H, H-4/9), 1.99−1.95 (m, 2H, H-8), 1.70 (s, 3H, H-20), 1.68−1.67 (m, 3H, H-1), 1.66 (s, 3H, H-19), 1.60 (s, 6H, H-17/18); **^{13}C NMR** (100 MHz, $CDCl_3$): δ (ppm) = 140.4 (C-10), 136.3 (C-14), 135.4 (C-6), 131.5 (C-2), 126.0 (C-15), 124.5 (C-3), 124.0 (C-7), 120.9 (C-11), 75.3 (C-13), 66.6 (C-12), 59.3 (C-16), 39.9 (C-8), 39.8 (C-4), 26.9 (C-9), 26.5 (C-5), 25.8 (C-1), 17.8 (C-17), 16.7 (C-19), 16.2 (C-18), 14.2 (C-20); **HRMS** (ESI) m/z calcd for $C_{20}H_{34}O_2Na^+$ $[M + Na]^+$, 329.2457; found, 329.2462.

*(2E,6E)-8-(((E)-3,7-Dimethylocta-2,6-dien-1-yl)oxy)-3,7-dimethylocta-2,6-dien-1-ol (**28**).* After deprotection of com-

https://doi.org/10.1021/acscatal.5c00272
ACS Catal. 2025, 15, 6796−6811

pound **25** (400 mg, 1.02 mmol), ether **28** (254 mg, 0.829 mmol, 81%) was obtained as a light yellow oil after column chromatography (PE/EtOAc = 5:1 → 4.5:1).

R_f (PE/EtOAc = 1:1): 0.49; **^{1}H NMR** (400 MHz, $CDCl_3$): δ (ppm) = 5.44−5.39 (m, 1H, H-15), 5.40−5.36 (m, 1H, H-11), 5.37−5.32 (m, 1H, H-7), 5.10 (tqui, J = 7.0, 1.4 Hz, 1H, H-3), 4.15 (ddq, J = 12.3, 6.3, 0.8 Hz, 2H, H-16), 3.92 (ddq, J = 12.3, 7.2, 0.6 Hz, 2H, H-8), 3.83 (br s, 2H, H-9), 2.20−2.14 (m, 2H, H-12), 2.12−2.07 (m, 4H, H-4/13), 2.05−2.01 (m, 2H, H-5), 1.69 (s, 3H, H-20), 1.68 (s, 3H, H-1), 1.65 (br s, 6H, H-19/18), 1.60 (br s, 3H, H-17); **^{13}C NMR** (100 MHz, $CDCl_3$): δ (ppm) = 140.1 (C-6), 139.5 (C-14), 133.0 (C-10), 131.8 (C-2), 127.6 (C-11), 124.2 (C-3), 123.8 (C-15), 121.3 (C-7), 75.2 (C-9), 66.1 (C-8), 59.5 (C-16), 39.8 (C-5), 39.3 (C-13), 26.5 (C-4), 26.1 (C-12), 25.8 (C-1), 17.8 (C-17), 16.6 (C-18), 16.4 (C-20), 14.2 (C-19); **HRMS** (ESI) m/z calcd for $C_{20}H_{34}O_2Na^+$ $[M + Na]^+$, 329.2457; found, 329.2457.

*(2E,6E,10E)-3,7,11-Trimethyl-12-((3-methylbut-2-en-1-yl)-oxy)dodeca-2,6,10-trien-1-ol (**29**).* After deprotection of compound **26** (489 mg, 1.25 mmol), ether **29** (316 mg, 1.03 mmol, 83%) was obtained as a light-yellow oil after column chromatography (PE/EtOAc = 5:1 → 4.5:1).

R_f (PE/EtOAc = 1:1): 0.47; **^{1}H NMR** (500 MHz, $CDCl_3$): δ (ppm) = 5.43−5.38 (m, 1H, H-7), 5.40−5.36 (m, 1H, H-15), 5.37−5.33 (m, 1H, H-3), 5.11−5.07 (m, 1H, H-11), 4.14 (d, J = 6.9 Hz, 2H, H-5), 3.88 (d, J = 6.9 Hz, 2H, H-4), 3.82 (s, 2H, H-16), 2.15−2.07 (m, 4H, H-13/9), 2.05−2.00 (m, 4H, H-8/12), 1.74 (s, 3H, H-1), 1.67 (s, 3H, H-18), 1.66 (s, 3H, H-17), 1.64 (s, 3H, H-20), 1.60 (s, 3H, H-19); **^{13}C NMR** (126 MHz, $CDCl_3$): δ (ppm) = 139.8 (C-6), 136.8 (C-2), 135.2 (C-10), 132.4 (C-14), 128.0 (C-15), 124.1 (C-11), 123.6 (C-7), 121.5 (C-3), 76.3 (C-16), 66.0 (C-4), 59.5 (C-5), 39.6 (C-8), 39.4 (C-12), 26.5 (C-9/13), 26.4 (C-9/13), 25.9 (C-1), 18.1 (C-17), 16.4 (C-18), 16.1 (C-19), 14.1 (C-20); **HRMS** (ESI) m/z calcd for $C_{20}H_{34}O_2Na^+$ $[M + Na]^+$, 329.2457; found, 329.2450.

*General Procedure for Pyrophosphorylation (Products **9**−**11**).* NCS (1.1 equiv) was dissolved in dry CH_2Cl_2 (0.4 M) and cooled to −30 °C. After dropwise addition of Me_2S (1.2 equiv), the solution was stirred at 0 °C for 5 min and then cooled to −40 °C. After the slow addition of the corresponding alcohol (1.0 equiv) in CH_2Cl_2 (0.5 M), the reaction mixture was stirred at 0 °C for 1.5 h and then at rt for 30 min. The reaction was terminated by addition of brine, followed by phase separation. The aqueous phase was extracted with Et_2O (3×). The combined organic phases were washed twice with brine, dried and the solvent was removed under reduced pressure. The chloride was obtained as an oil and used in the subsequent reaction without further purification.

A solution of the chloride (1.0 equiv) in MeCN (0.1 M) was added dropwise to a suspension of $(n\mathrm{Bu}_4\mathrm{N})_3\mathrm{HP}_2\mathrm{O}_7$ (1.8 equiv) in MeCN (0.1 M). The reaction mixture was stirred at rt for 18 h and then the solvent was removed under reduced pressure. The residue was taken up in an ion exchange buffer (25 mM NH_4HCO_3 in 2% iPrOH) and transformed into the ammonium salt using an ion exchange [DOWEX AG 50W-X8 (100−200 mesh; NH_4^+ form)]. The elution was monitored by checking the pH-value (pH 8.0 → 6.5). After lyophilization of the eluate, the inorganic diphosphate salt was precipitated by dissolving the solid in 5 mL of 0.05 M NH_4HCO_3 solution and adding 15 mL of a MeCN/*i*PrOH mixture (1:1). The mixture was gently shaken and centrifuged at 5000 rpm for 10 min. The supernatant was separated and the precipitate was resuspended in 5 mL of a 0.05 M NH_4HCO_3 solution. The procedure was repeated twice and the combined supernatants were concentrated under reduced pressure.

*Trisammonium (E)-3-methyl-4-(((2E,6E)-3,7,11-trimethyl-dodeca-2,6,10-trien-1-yl)oxy)but-2-en-1-yldiphosphate (**9**).* The corresponding pyrophosphate **9** (188 mg, 0.363 mmol, 89% o2s) was obtained from alcohol **27** (125 mg, 0.408 mmol) as a light-yellow powder.

^{1}H NMR (400 MHz, D_2O): δ (ppm) = 5.69 (t, J = 6.0 Hz, 1H, H-15), 5.36 (t, J = 7.1 Hz, 1H, H-11), 5.18 (t, J = 6.6 Hz, 1H, H-7), 5.16 (t, J = 7.2 Hz, 1H, H-3), 4.55 (t, J = 6.4 Hz, 2H, H-16), 4.03 (d, J = 7.1 Hz, 2H, H-12), 3.95 (s, 2H, H-13), 2.17−2.14 (m, 2H, H-8), 2.11−2.08 (m, 4H, H-4/9), 2.03−1.99 (m, 2H, H-5), 1.72 (s, 3H, H-20), 1.69 (s, 3H, H-19), 1.68 (s, 3H, H-1) 1.61 (s, 6H, H-17/18); **^{13}C NMR** (100 MHz, D_2O): δ (ppm) = 142.7 (C-10), 136.9 (C-14), 136.2 (C-6), 132.9 (C-2), 124.4 (C-3), 124.2 (C-7), 123.8 (d, C-15), 119.6 (C-11), 74.6 (C-13), 65.8 (C-12), 62.3 (d, C-16), 38.9 (2C, C-5/9), 25.9 (C-4), 25.5 (C-8), 24.9 (C-1), 17.0 (C-17), 15.6 (C-19), 15.4 (C-18), 13.5 (C-20); **^{31}P NMR** (162 MHz, D_2O): δ (ppm) = −9.14 (d, J = 20.8 Hz), −10.22 (d, J = 20.8 Hz); **HRMS** (ESI) m/z calcd for $C_{20}H_{36}O_8P_2^-$ $[M-H]^-$, 465.1807; found, 465.1813.

*Trisammonium (2E,6E)-8-(((E)-3,7-dimethylocta-2,6-dien-1-yl)oxy)-3,7-dimethylocta-2,6-dien-1-yldiphosphate (**10**).* The corresponding pyrophosphate **10** (180 mg, 0.345 mmol, 72% o2s) was obtained from alcohol **28** (148 mg, 0.483 mmol) as a light-yellow powder.

^{1}H NMR (400 MHz, D_2O): δ (ppm) = 5.51−5.46 (m, 2H, H-11), 5.34 (tsxt, J = 7.2, 1.2 Hz, 1H, H-7), 5.19 (tqui, J = 6.8, 1.3 Hz, 2H, H-3), 4.48 (t, J = 6.2 Hz, 2H, H-16), 3.98 (d, J = 7.2 Hz, 2H, H-8), 3.91 (s, 2H, H-9), 2.26−2.20 (m, 2H, H-12), 2.18−2.09 (m, 6H, H-4/13/5), 1.74 (s, 3H, H-20), 1.69 (m, 3H, H-1), 1.68 (m, 3H, H-18) 1.66 (s, 3H, H-19), 1.63 (s, 3H, H-17); **^{13}C NMR** (100 MHz, D_2O): δ (ppm) = 142.9 (C-6), 142.4 (C-14), 133.5 (C-2), 131.9 (C-10), 129.7 (C-11), 124.2 (C-3), 120.0 (d, C-15), 119.5 (C-7), 75.3 (C-9), 64.9 (C-8), 62.4 (d, C-16), 38.7 (C-5), 38.4 (C-13), 25.5 (C-12), 25.4 (C-4), 24.8 (C-1), 17.0 (C-17), 15.6 (C-20), 15.5 (C-18), 13.3 (C-19); **^{31}P NMR** (162 MHz, D_2O): δ (ppm) = −6.40 (d, J = 20.0 Hz), −10.07 (d, J = 20.0 Hz); **HRMS** (ESI) m/z calcd for $C_{20}H_{36}O_8P_2^-$ $[M-H]^-$, 465.1807; found, 465.1808.

*Trisammonium (2E,6E,10E)-3,7,11-trimethyl-12-((3-methylbut-2-en-1-yl)oxy)dodeca-2,6,10-trien-1-yldiphosphate (**11**).* The corresponding pyrophosphate **11** (127 mg, 0.246 mmol, 61% o2s) was obtained from alcohol **29** (124 mg, 0.403 mmol) as a light-yellow powder.

^{1}H NMR (400 MHz, D_2O): δ (ppm) = 5.47−5.43 (m, 2H, H-15/7), 5.35 (tspt, J = 7.4, 1.4 Hz, 1H, H-3), 5.23−5.20 (m, 1H, H-11), 4.46 (dd, J = 6.4 Hz, 2H, H-16), 3.91 (d, J = 7.4 Hz, 2H, H-4), 3.90 (s, 2H, H-5), 2.23−2.17 (m, 2H, H-13), 2.15−2.05 (m, 6H, H-9/8/12), 1.75 (s, 3H, H-1), 1.71 (s, 3H, H-20), 1.68 (s, 3H, H-17), 1.63 (br s, 6H, H-18/19); **^{13}C NMR** (100 MHz, D_2O): δ (ppm) = 142.7 (C-14), 140.3 (C-2), 136.2 (C-10), 131.5 (C-6), 130.1 (C-7), 124.5 (C-11), 119.8 (d, J = 8.7 Hz, C-15), 119.1 (C-3), 75.8 (C-5), 64.8 (C-4), 62.4 (d, J = 5.2 Hz, C-16), 38.8 (C-12), 38.3 (C-8), 25.7 (C-9), 25.4 (C-13), 24.9 (C-1), 17.2 (C-17), 15.6 (C-20), 15.1 (C-19), 13.2 (C-18); **^{31}P NMR** (162 MHz, D_2O): δ (ppm) = −6.10 (d, J = 21.1 Hz), −9.95 (d, J = 21.1 Hz); **HRMS** (ESI) m/z cacld for $C_{20}H_{36}O_8P_2^-$ $[M-H]^-$, 465.1807; found, 465.1801.

Biological Experiments. *Genes, Strains, Plasmids and Growth Conditions.* The genes used in this work were optimized for expression in *E. coli* and synthesized by GenScript Biotech(Netherlands)B.V. as constructs in pET28a(+) and

https://doi.org/10.1021/acscatal.5c00272
ACS Catal. 2025, 15, 6796−6811

pET28a(+)-TEV, respectively. TXS and PvHVS were expressed in an N-terminal truncated form, corresponding to the deletion of 60 and 47 amino acids of the preproteins, respectively, for better solubility.[12,15] PaFS is a bifunctional enzyme and only its DTS domain was expressed, corresponding to 350 N-terminal amino acids.[10] *E. coli* cultures were grown at 37 °C and 180 rpm in Luria−Bertani medium (LB medium: 0.5% yeast extract, 1% tryptone/peptone, 0.05% sodium chloride) supplemented with 50 μg-mL-1 kanamycin. For heterologous expression, 2TY medium (1% yeast extract, 1.6% tryptone/peptone, 0.5% sodium chloride) supplemented with 50 $\mu g \cdot mL^{-1}$ kanamycin was inoculated from a 2% preculture of *E. coli* BL21 (DE3) and grown at 37 °C and 180 rpm to an optical density (OD_{600}) of 0.4−0.6. T7lac promoter-driven expression was then induced by the addition of 0.5 mM IPTG (isopropyl-β-thiogalactopyranoside) and the temperature was lowered to 16 °C for overnight cultivation.

Protein Purification. The diterpene synthases were overexpressed as described above. After harvesting, the cells were suspended in lysis buffer (100 mM Tris, 40 mM NaCl, 25 mM imidazole, pH 8.0), disrupted by sonication (sonotrode: KE76, *I* = 45%, 10s/10s) and the histidine-tagged protein was purified by affinity chromatography. For this purpose, Protino Ni-NTA agarose (Macherey-Nagel GmbH & Co. KG) was used for small amounts of protein, while large amounts were purified using ÄKTA pure 25L with a HisTrap FF column (GE Healthcare). Protein concentrations were determined by UV/vis spectroscopy.

Enzyme Purification and Yield. Heterologous expression under the above-mentioned conditions and protein purification by FPLC System Äkta pure (GE Healthcare, Chicago, USA) with a Ni-NTA column (HiTrap IMAC FF 5 mL, Ni^{2+}) gave an average enzyme yield of 200 mg/L culture for CotB2, 120 mg/L for PvHVS and 100 mg/L for $PaFS_{350}$, respectively.

Enzyme Assays. Enzyme assays were performed in 0.5 mL scale in HEPES buffer (50 mM, pH 7.5 for CotB2, PvHVS and Bnd4, pH 8.0 for TXS, $PaFS_{350}$ and PaFS) with DTT (dithiothreitol, 5 mM). The purified enzyme was transferred to the chosen buffer by gel filtration using PD-10 desalting columns (GE Healthcare) and used at a concentration of 0.01 $g \cdot L^{-1}$. GGPP (geranylgeranyl pyrophosphate) or unnatural substrate was then added at concentrations of 150 μM and $MgCl_2$ (5 mM). After incubation at 30 °C (ThermoMixer) for 20 min, the samples were extracted with 100 μL *n*-hexane. The extracts were analyzed by GC/MS.

Temperature Optimization of Biotransformations with GGPP Ethers as Substrate. All optimizations were performed in triplicate with geranylgeraniol as internal standard for semiquantification. First, a general optimization was carried out with corresponding well-accepted GGPP ethers as substrate. The optimization was aimed at improving the yield of the main cyclization product.

As previously shown, the extraction procedure requires at least 100 μL of *n*-hexane, a single extraction and an extraction time of 30 s for the product to be completely transferred to the organic phase. Longer extraction times and larger volumes did not result in higher yields. Furthermore, multistep extraction revealed that no additional product could be recovered after the second extraction step.[12]

The temperature was optimized by testing a range between 10 and 40 °C (ThermoMixer). The enzymes showed the highest activity between 25 and 30 °C. A higher temperature of 30 °C was chosen for all semipreparative biotransformations for better analogue acceptance.

Enzymatic Conversion of 9 with CotB2. Semipreparative biotransformation with GGPP ether analogue **9** (140.4 mg, 312.4 μmol, 1.5 mM, each biotransformation contains 34−36 mg) was performed in HEPES buffer (50 mM, pH 7.5) supplemented with DTT (5 mM) and 10 mM $MgCl_2$. The enzyme CotB2 was purified by IMAC as described above, transferred to 50 mM HEPES buffer and utilized in a concentration of 0.1 $g \cdot L^{-1}$. Tween20 (0.02% [v/v]) and pyrophosphatase (1U) (from *Streptomyces cerevisiae*) were added to prevent substrate precipitation or enzyme inhibition by inorganic diphosphate. The mixture was incubated at 30 °C and 40 rpm for 24 h. After 3 and 6 h, fresh CotB2 and $MgCl_2$ (10 mM after 6 h) were added to the assay. The GGPP ether analogue **9** was added continuously (250 μM/h) over 5 h. After the incubation the aqueous mixture was extracted with *n*-pentane/MTBE (1:1, 3 times). The combined organic phases were washed excessively with brine, dried with $MgSO_4$ and filtered. After removal of the solvent, a yellowish and waxy crude product was collected (90.5 mg). The main product **30** (6.8 mg, 23.6 μmol, 7.6%) was isolated by column chromatography (*n*-pentane/diethyl ether = 5:1). After solvent evaporation under reduced pressure the product was further purified by SP-NP-HPLC [*n*-hexane/*n*-hexane:*i*PrOH 5%; 0% (iso 2 min) 0% → 50% (74 min)−50% → 100% (4 min)−100% (iso 10 min); t_R = 8.64 min]. The product was concentrated under a stream of argon and the solvent was coevaporated with C_6D_6.

$RI_{DB\text{-}5HT}$: 2251; **RI_{WAX}**: 2714; **HR-GC-MS** (CI) *m*/*z* calcd for $C_{20}H_{32}O$, 288.2453; found, 288.2452; **^{1}H NMR** (500 MHz, C_6D_6): δ (ppm) = 6.22 (br s), 5.57 (t, *J* = 8.1 Hz, 1H), 4.05 (dd, *J* = 11.2, 1.5 Hz, 1H), 3.96 (dd, *J* = 11.2, 3.0 Hz, 1H), 2.69−2.66 (m, 1H), 2.56−2.50 (m, 1H), 2.11 (d, *J* = 1.0 Hz, 3H), 2.02−1.96 (m, 1H), 1.97−1.92 (?), 1.76 (dd, *J* = 13.8, 4.3 Hz, 1H), 1.75−1.70 (m, 1H), 1.53−1.49 (m, 1H), 1.50−1.44 (m, 1H), 1.42 (t, *J* = Hz, 3H), 1.40−1.33 (m, 1H), 1.34−1.26 (m, 2H), 1.01 (t, *J* = 13.8 Hz, 1H), 0.89 (d, *J* = 6.8 Hz, 3H), 0.79 (d, *J* = 6.8 Hz, 3H), 0.72 (s, 3H); **^{13}C NMR** (126 MHz, C_6D_6): δ (ppm) = 139.05, 135.85, 129.40, 110.60, 68.35, 55.53, 47.95, 44.33, 43.90, 40.87, 36.51, 35.61, 29.46, 24.14, 23.82, 23.79, 23.20, 20.29, 17.80, 16.66.

Enzymatic Conversion of 9 with PvHVS. Semipreparative biotransformation with GGPP ether analogue **9** (181.9 mg, 351.6 μmol, 1.5 mM, each biotransformation contains 36−37 mg) was performed in HEPES buffer (50 mM, pH 7.5) supplemented with DTT (5 mM) and 10 mM $MgCl_2$. The enzyme PvHVS was purified by IMAC as described above, transferred to 50 mM HEPES buffer and utilized in a concentration of 0.1 $g \cdot L^{-1}$. Tween20 (0.02% [v/v]) and pyrophosphatase (1U) (from *S. cerevisiae*) were added to prevent substrate precipitation or enzyme inhibition by inorganic diphosphate. The mixture was incubated at 30 °C and 40 rpm for 24 h. After 3 and 6 h, fresh PvHVS and $MgCl_2$ (10 mM after 6 h) were added to the assay. The GGPP ether analogue **9** was added continuously (250 μM/h) over 5 h. After the incubation the aqueous mixture was with *n*-pentane/MTBE (1:1, 3 times). The combined organic phases were washed excessively with brine, dried with $MgSO_4$ and filtered. After removal of the solvent, a yellowish and waxy crude product was collected (16.6 mg). The products **32** (1.1 mg, 3.59 μmol, 1.0%) and **31** were separated by column chromatography (*n*-pentane/MTBE = 20:1−10:1−3:2). After solvent evaporation under reduced pressure the product **31** was further purified by SP-NP-

https://doi.org/10.1021/acscatal.5c00272
ACS Catal. 2025, 15, 6796−6811

HPLC [*n*-hexane/*n*-hexane:*i*PrOH 1%; 0% (iso 10 min) 0% → 90% (70 min)−90% (iso 11 min)−100% (iso 9 min); t_R = 13.50 min] and then dissolved in C_6D_6.

$RI_{DB\text{-}5HT}$: 2043; **RI_{WAX}**: 2418; **HR-GC-MS** (CI) *m*/*z* calcd for $C_{20}H_{32}O$ 288.2453; found, 288.2451; **^{1}H NMR** (500 MHz, C_6D_6): δ (ppm) = 5.87 (dd, *J* = 18.0, 10.5 Hz, 1H), 5.25−5.22 (m, 1H), 5.24−5.21 (m, 1H), 4.99 (dd, *J* = 6.0, 1.4 Hz, 1H), 4.97 (s, 1H), 4.92 (q, *J* = 1.3 Hz, 1H), 4.86 (br s, 1H), 4.05 (dd, *J* = 8.5, 7.4 Hz, 1H), 3.96 (dd, *J* = 8.5, 7.4 Hz, 1H), 3.85 (d, *J* = 8.3 Hz, 1H), 3.50 (d, *J* = 8.3 Hz, 1H), 2.37 (t, *J* = 7.4 Hz, 1H), 2.19−2.14 (m, 2H), 2.15−2.11 (m, 2H), 2.08 (dd, *J* = 8.3, 6.7 Hz, 2H), 2.05−1.94 (m, 1H), 1.68 (m, 3H), 1.58 (s, 3H), 1.56 (s, 3H), 1.06 (s, 3H); **^{13}C NMR** (126 MHz, C_6D_6): δ (ppm) = 147.34, 141.72, 135.37, 131.24, 124.87, 124.49, 113.03, 111.31, 78.86, 72.30, 56.08, 48.09, 40.18, 37.18, 27.16, 26.81, 25.88, 23.49, 17.77, 16.12.

Product **32** was isolated by column chromatography (*n*-pentane/MTBE = 20:1−10:1−3:2). After solvent evaporation under reduced pressure, the purified product was dissolved in C_6D_6.

$RI_{DB\text{-}5HT}$: 2243; **RI_{WAX}**: 2901; **HRMS** (ESI) *m*/*z* calcd for $C_{20}H_{34}O_2Na$ $[M + Na]^+$, 329.2457; found, 329.2449; **^{1}H NMR** (600 MHz, C_6D_6): δ (ppm) = 6.36 (dd, *J* = 17.8, 10.9 Hz, 1H), 5.24 (tspt, *J* = 7.0, 1.4 Hz, 1H), 5.21 (tsxt, *J* = 7.2, 1.3 Hz, 1H), 4.96 (dd, *J* = 17.8, 1.5 Hz, 1H), 4.93 (dd, *J* = 10.9, 1.5 Hz, 1H), 4.32 (dd, *J* = 9.5, 8.4 Hz, 1H), 4.08 (dd, *J* = 9.2, 8.4 Hz, 1H), 3.62 (d, *J* = 8.2 Hz, 1H), 3.39 (d, *J* = 8.2 Hz, 1H), 2.20−2.16 (m, 2H), 2.15−2.07 (m, 1H), 2.10−2.07 (m, 2H), 2.02−1.96 (m, 1H), 1.89 (t, *J* = 9.3 Hz, 1H), 1.69 (m, 3H), 1.61 (br s, 3H), 1.57 (br s, 3H), 1.43−1.38 (m, 1H), 1.31−1.26 (m, 1H), 1.12 (s, 3H), 0.98 (s, 3H); **^{13}C NMR** (151 MHz, C_6D_6): δ (ppm) = 143.15, 135.18, 131.32, 124.97, 124.86, 112.69, 81.39, 73.42, 69.55, 58.39, 47.04, 42.81, 40.20, 27.16, 25.97, 25.89, 22.84, 22.14, 17.78, 16.05.

*Enzymatic Conversion of **10** with $PaFS_{350}$.* Semipreparative biotransformation with GGPP ether analogue **10** (190.7 mg, 368.7 μmol, 1.5 mM, each biotransformation contains 47−48 mg) was performed in HEPES buffer (50 mM, pH 8.0) supplemented with DTT (5 mM) and 10 mM $MgCl_2$. The enzyme $PaFS_{350}$ was purified by IMAC as described above, transferred to 50 mM HEPES buffer and utilized in a concentration of 0.1 g·L^{-1}. Tween20 (0.02% [v/v]) and pyrophosphatase (1U) (from *S. cerevisiae*) were added to prevent substrate precipitation or enzyme inhibition by inorganic diphosphate. The mixture was incubated at 30 °C and 40 rpm for 24 h. After 3 and 6 h, fresh $PaFS_{350}$ and $MgCl_2$ (10 mM after 6 h) were added to the assay. The GGPP ether analogue **10** was added continuously (250 μM/h) over 5 h. After incubation the aqueous mixture was extracted with *n*-pentane/MTBE (2:1, 3 times). The combined organic phases were washed excessively with brine, dried with $MgSO_4$ and filtered. After removal of the solvent, a yellowish and waxy oil (74.4 mg) was collected and after purification by column chromatography (*n*-pentane/MTBE = 1:0−2:1) the product **33** (9.0 mg, 29.4 μmol, 8.0%) was isolated as a mixture of diastereomers (dr = 2:1, determined by GC). After solvent evaporation under reduced pressure, it was further purified by SP-NP-HPLC [*n*-hexane/*n*-hexane:*i*PrOH 1%; 0% (iso 10 min) 0% → 20% (70 min)−100% (iso 20 min); t_R = 43.07 min] and the solvent was removed under a stream of nitrogen. The residue was dissolved in C_6D_6.

$RI_{DB\text{-}5HT}$: 2298 (**33**); **RI_{WAX}**: 2752 (**33a**), 2767 (**33b**); **HR-GC-MS** (**33**, CI) *m*/*z* calcd for $C_{20}H_{34}O_2$ 306.2559; found, 306.2563; (**33a**, 298 K): **^{1}H NMR** (600 MHz, C_6D_6): δ (ppm) = 5.33 (tspt, *J* = 7.1, 1.4 Hz, 1H), 5.03 (t, *J* = 7.5 Hz, 1H), 4.89 (t, *J* = 7.1 Hz, 1H), 3.94 (d, *J* = 11.7 Hz, 1H), 3.78 (dd, *J* = 11.0, 8.4 Hz, 1H), 3.55−3.50 (m, 1H), 3.18 (dd, *J* = 11.9, 1.1 Hz, 1H), 2.42−2.32 (m, 2H), 2.03−2.00 (m, 1H), 2.02−1.98 (m, 1H), 2.02−1.91 (m, 2H), 1.95−1.89 (m, 1H), 1.74 (ddd, *J* = 13.6, 11.3, 5.4 Hz, 1H), 1.70−1.69 (m, 3H), 1.66 (d, *J* = 0.5 Hz, 3H), 1.61 (ddd, *J* = 13.6, 11.3, 5.4 Hz, 1H), 1.58−1.52 (m, 1H), 1.50 (d, *J* = 0.9 Hz, 3H), 1.42 (s, 3H), 1.14 (s, 3H); **^{13}C NMR** (126 MHz, C_6D_6): δ (ppm) = 134.23, 132.71, 132.42, 130.96, 126.90, 125.87, 78.43, 74.41, 66.75, 41.64, 39.22, 25.97, 25.94, 25.48, 23.67, 22.81, 17.78, 15.44, 14.88.

(**33a**, 333 K): **^{1}H NMR** (600 MHz, C_6D_6): δ (ppm) = 5.31 (tspt, *J* = 7.1, 1.4 Hz, 1H), 5.05 (t, *J* = 7.2 Hz, 1H), 4.95 (t, *J* = 7.3 Hz, 1H), 3.95 (d, *J* = 11.5 Hz, 1H), 3.76 (dd, *J* = 12.0, 7.2 Hz, 1H), 3.54 (d, *J* = 11.5 Hz, 1H), 3.21 (dd, *J* = 12.0, 1.2 Hz, 1H), 2.34−2.29 (m, 2H), 2.07−2.00 (m, 1H), 2.05−1.93 (m, 2H), 2.04−1.99 (m, 1H), 1.95−1.92 (m, 1H), 1.74−1.67 (m, 1H), 1.69 (m, 3H), 1.65 (m, 3H), 1.63−1.56 (m, 1H), 1.59−1.54 (m, 1H), 1.52 (d, *J* = 1.1 Hz, 3H), 1.52−1.46 (m, 1H), 1.44 (br t, *J* = 0.9, 3H), 1.14 (s, 3H); **^{13}C NMR** (126 MHz, C_6D_6): δ (ppm) = 134.09, 132.50, 132.44, 130.91, 127.16, 125.98, 78.48, 74.42, 66.84, 51.18, 41.58, 39.29, 26.40, 25.79, 25.45, 23.92, 22.91, 17.72, 15.46, 14.97.

(**33b**, 298 K): **^{1}H NMR** (600 MHz, C_6D_6): δ (ppm) = 5.31 (tspt, *J* = 7.1, 1.4 Hz, 1H), 5.05 (t, *J* = 7.5 Hz, 1H), 4.92 (t, *J* = 7.1 Hz, 1H), 3.96 (d, *J* = 11.7 Hz, 1H), 3.71−3.65 (m, 1H), 3.57−3.52 (m, 1H), 3.16 (d, *J* = 10.7 Hz, 1H), 2.47−2.42 (m, 1H), 2.24−2.17 (m, 1H), 2.19−2.16 (dd, *J* = 10.3, 7.1 Hz, 2H), 2.07−2.02 (m, 1H), 2.04−1.90 (m, 2H), 1.98−1.92 (m, 1H), 1.70−1.69 (m, 3H), 1.69 (ddd, *J* = 13.5, 11.8, 4.8 Hz), 1.64 (d, *J* = 0.5 Hz, 3H), 1.55−1.50 (m, 1H), 1.52 (d, *J* = 0.9 Hz, 3H), 1.51−1.47 (m, 1H), 1.44 (s, 3H), 1.22 (s, 3H); **^{13}C NMR** (126 MHz, C_6D_6): δ (ppm) = 134.09, 132.30, 132.19, 130.99, 127.24, 125.93, 78.79, 74.37, 67.04, 39.80, 39.22, 25.93, 25.82, 25.47, 25.37, 22.90, 17.77, 15.40, 14.96.

(**33b**, 333 K): **^{1}H NMR** (600 MHz, C_6D_6): δ (ppm) = 5.29 (tspt, *J* = 7.2, 1.4 Hz, 1H), 5.07 (t, *J* = 7.2 Hz, 1H), 4.98 (t, *J* = 7.3 Hz, 1H), 3.96 (d, *J* = 11.5 Hz, 1H), 3.66 (dd, *J* = 12.2, 6.8 Hz, 1H), 3.55 (d, *J* = 11.5 Hz, 1H), 3.19 (dd, *J* = 12.2, 1.1 Hz, 1H), 2.39−2.26 (m, 1H), 2.21−2.15 (m, 1H), 2.20−2.15 (m, 1H), 2.06−2.02 (m, 1H), 2.05−1.93 (m, 2H), 1.98−1.93 (m, 1H), 1.70−1.64 (m, 1H), 1.68 (m, 3H), 1.63 (m, 3H), 1.58−1.53 (m, 1H), 1.56−1.52 (m, 1H), 1.54−1.48 (m, 1H), 1.53 (d, *J* = 1.1 Hz, 3H), 1.45 (br t, *J* = 0.9 Hz, 3H), 1.21 (s, 3H); **^{13}C NMR** (126 MHz, C_6D_6): δ (ppm) = 133.97, 132.65, 132.11, 130.96, 127.46, 126.00, 78.37, 74.43, 67.20, 52.05, 40.13, 39.29, 26.10, 25.80, 25.46, 25.36, 22.99, 17.72, 15.44, 15.05.

*Enzymatic Conversion of **11** with $PaFS_{350}$.* Semipreparative biotransformation with GGPP ether analogue **11** (74.7 mg, 144.4 μmol, 1.5 mM, each biotransformation contains 36−37 mg) was performed in HEPES buffer (50 mM, pH 8.0) supplemented with DTT (5 mM) and 10 mM $MgCl_2$. The enzyme $PaFS_{350}$ was purified by IMAC as described above, transferred to 50 mM HEPES buffer and utilized in a concentration of 0.1 g·L^{-1}. Tween20 (0.02% [v/v]) and pyrophosphatase (1U) (from *S. cerevisiae*) were added to prevent substrate precipitation or enzyme inhibition by inorganic diphosphate. The mixture was incubated at 30 °C and 40 rpm for 24 h. After 3 and 6 h, fresh $PaFS_{350}$ and $MgCl_2$ (10 mM after 6 h) were added to the assay. The GGPP ether analogue **11** was added continuously (250 μM/h) over 5 h. After incubation the aqueous mixture was extracted with *n*-pentane/MTBE (1:1, 3 times). The combined organic phases were

https://doi.org/10.1021/acscatal.5c00272
ACS Catal. 2025, 15, 6796−6811

washed excessively with brine, dried with $MgSO_4$ and filtered. After removal of the solvent, a yellowish and waxy crude product was collected (15.9 mg). The products **34** and **35** were isolated by column chromatography (*n*-pentane/MTBE = 1:0−2:1). **34** was isolated after solvent evaporation under a stream of nitrogen the product was further purified by SP-NP-HPLC [*n*-hexane/*n*-hexane:*i*PrOH 1%; 0% (iso 10 min) 0% → 20% (70 min)−100% (iso 20 min); t_R = 8.35 min] and P-NP-HPLC (100% *n*-hexane; t_R = 7.25 min). The isolated product was concentrated under a stream of argon and the solvent was coevaporated with C_6D_6.

34: $\mathbf{RI}_{\text{DB-5HT}}$: 2080; RI_{WAX}: 2444; **HR-GC-MS** (CI) *m*/*z* calcd for $C_{20}H_{33}O$ $[M + H]^+$, 289.2531; found, 289.2545; **^{1}H NMR** (600 MHz, C_6D_6): δ (ppm) = 5.53 (tspt, *J* = 10.1, 1.3 Hz, 1H), 5.12−5.08 (m, 1H), 4.86−4.84 (m, 2H), 4.03 (d, *J* = 6.6 Hz, 2H), 3.33 (dd, *J* = 20.4, 8.7 Hz, 2H), 2.88 (dt, *J* = 14.4, 8.7 Hz, 1H), 2.42−2.38 (m, 1H), 2.41−2.38 (m, 1H), 2.30 (ddt, *J* = 12.0, 11.6, 7.4 Hz, 1H), 2.06−2.03 (m, 1H), 1.97−1.92 (m, 1H), 1.93−1.88 (m, 1H), 1.97 (ddd, *J* = 11.4, 8.6, 2.9 Hz, 1H), 1.74 (t, *J* = 11.4 Hz, 1H), 1.67−1.61 (m, 1H), 1.61−1.60 (m, 3H), 1.55 (br s, 3H), 1.55−1.48 (m, 1H), 1.54 (br s, 3H), 1.40−1.35 (m, 1H), 1.08 (s, 3H); **^{13}C NMR** (126 MHz, C_6D_6): δ (ppm) = 149.97, 136.28, 135.33, 122.90, 122.29, 113.18, 79.18, 68.24, 49.62, 43.74, 41.97, 39.61, 37.34, 35.63, 27.47, 25.75, 25.44, 21.20, 18.86, 18.07.

35 was isolated After solvent evaporation under a stream of nitrogen the product was further purified by SP-NP-HPLC [*n*-hexane/*n*-hexane:*i*PrOH 1%; 0% (iso 10 min) 0% → 20% (70 min)−100% (iso 20 min); t_R = 8.35 min] and P-NP-HPLC (100% *n*-hexane; t_R = 6.57 min). The isolated product was concentrated under a stream of argon and the solvent was coevaporated with C_6D_6.

$\mathbf{RI}_{\text{DB-5HT}}$: 1966; RI_{WAX}: 2243; **HR-GC-MS** (EI) *m*/*z* calcd for $C_{20}H_{32}O$, 288.2453; found, 288.2463; **^{1}H NMR** (600 MHz, C_6D_6): δ (ppm) = 5.53−5.49 (m, 1H), 3.95 (dd, *J* = 6.6 Hz, 2H), 3.05 (d, *J* = 20.2, 8.6 Hz, 2H), 2.40−2.38 (m, 2H), 2.17−2.15 (m, 1H), 2.16−2.13 (m, 2H), 2.03−2.00 (m, 1H), 1.91−1.83 (m, 2H), 1.68−1.67 (m, 3H), 1.61−1.60 (m, 3H), 1.51 (br s, 3H), 1.16 (dd, *J* = 14.6, 11.4 Hz 1H), 1.11 (s, 3H), 0.92 (s, 3H), 0.59 (dd, *J* = 8.4, 4.0 Hz, 1H), 0.51 (ddt, *J* = 11.2, 8.3, 5.5 Hz, 1H), 0.24 (t, *J* = 4.4 Hz, 1H); **^{13}C NMR** (151 MHz, C_6D_6): δ (ppm) = 136.31, 135.13, 132.71, 122.91, 80.97, 68.24, 53.84, 39.14, 38.29, 38.19, 38.09, 26.77, 25.73, 22.94, 22.42, 21.54, 20.67, 20.54, 18.02, 13.97.

*Enzymatic Conversion **50** by PvHVS.* Semipreparative biotransformation with FPP ether derivative **50** (138 mg, 307 μmol, 1.5 mM, 6 flasks à 23 mg) was performed in HEPES buffer (50 mM, pH 7.5) supplemented with DTT (5 mM) and 10 mM $MgCl_2$. The enzyme PvHVS was purified by IMAC as described above, transferred to 50 mM HEPES buffer and utilized in a concentration of 0.1 g·L^{-1}. Tween20 (0.02% [v/v]) and pyrophosphatase (1U) (from *S. cerevisiae*) were added to prevent substrate precipitation or enzyme inhibition by inorganic diphosphate. From a 14 mM pyrophosphate in 10% aq. NH_4HCO_3 solution, 0.5 mL was added to each preparation every 30 min over a period of 3−4 h. The mixture was incubated at 29 °C and at 50 rpm over a period of 24 h. After incubation the aqueous mixture was extracted with *n*-pentane (3×). The combined organic phases were washed excessively with brine, dried over $MgSO_4$ and concentrated under reduce pressure and in a stream of argon. The product **51** was isolated by column chromatography (Et_2O/*n*-pentane 0−25%) and the products **52** and **53** were separated by SP-NP-HPLC (details see below).

51 was isolated product was concentrated under a stream of argon and the solvent was coevaporated with C_6D_6.

$\mathbf{RI}_{\text{DB-5HT}}$: 1757; **HR-GC-MS** (CI) *m*/*z* calcd for $C_{15}H_{25}O^+$ $(M\text{-}H_2O + H)^+$, 221.1905; found, 221.1904; **^{1}H NMR** (600 MHz, C_6D_6): δ (ppm) = 6.35 (dd, *J* = 17.8, 10.9 Hz, 1H), 5.15 (t, *J* = 7.2 Hz, 1H), 4.94 (dd, *J* = 17.8, 1.6 Hz, 1H), 4.87 (dd, *J* = 10.9, 1.6 Hz, 1H), 4.32 (t, *J* = 9.0 Hz, 1H), 4.08 (t, *J* = 8.7 Hz, 1H), 3.62 (d, *J* = 8.2 Hz, 1H), 3.39 (d, *J* = 8.2 Hz, 1H), 2.15−2.04 (m, 1H), 2.01−1.92 (m, 1H), 1.89 (t, *J* = 9.3 Hz, 1H), 1.66 (s, 3H), 1.56 (s, 3H), 1.38 (t, *J* = 2.6 Hz, 1H), 1.29 (t, *J* = 5.2 Hz, 1H), 1.11 (s, 3H), 0.98 (s, 3H); **^{13}C NMR** (151 MHz, C_6D_6): δ (ppm) = 143.15, 131.34, 125.05, 112.71, 81.39, 73.39, 69.55, 58.40, 47.04, 42.85, 25.96, 25.84, 22.92, 22.14, 17.66.

Product **52** was isolated by SP-NP-HPLC [*n*-hexane/*n*-hexane:*i*PrOH 5%; 0% (iso 10 min) 0% → 5% (70 min)−5% (iso 11 min)−100% (iso 9 min); t_R = 30 min]. The isolated product was concentrated under a stream of argon and the solvent was coevaporated with C_6D_6.

$\mathbf{RI}_{\text{DB-5HT}}$: 1680; **HR-GC-MS** (CI) *m*/*z* calcd for $C_{15}H_{25}O^+$ $(M + H)^+$, 221.1905; found, 221.1904; **^{1}H NMR** (600 MHz, C_6D_6): δ (ppm) = 5.88 (dd, *J* = 17.6, 10.9 Hz, 1H), 5.26 (t, *J* = 7.1 Hz, 1H), 5.23−5.19 (m, 1H), 4.99−4.90 (m, 2H), 4.02−3.98 (m, 1H), 3.95 (dd, *J* = 8.7, 7.3 Hz, 1H), 3.86 (d, *J* = 8.3 Hz, 1H), 3.50 (d, *J* = 8.2 Hz, 1H), 2.73 (t, *J* = 7.1 Hz, 2H), 2.35 (t, *J* = 7.4 Hz, 1H), 1.66 (s, 3H), 1.54 (s, 3H), 1.54 (s, 3H), 1.04 (s, 3H); **^{13}C NMR** (151 MHz, C_6D_6): δ (ppm) = 142.09, 132.83, 131.47, 126.88, 123.60, 112.66, 78.71, 71.26, 59.19, 48.45, 27.47, 25.79, 23.92, 17.77, 16.35.

Product **53** was isolated by SP-NP-HPLC [*n*-hexane/*n*-hexane:*i*PrOH 5%; 0% (iso 10 min) 0% → 5% (70 min)−5% (iso 11 min)−100% (iso 9 min); t_R = 27 min]. The isolated product was concentrated under a stream of argon and the solvent was coevaporated with C_6D_6.

$\mathbf{RI}_{\text{DB-5HT}}$: 1564; **HR-GC-MS** (CI) *m*/*z* calcd for $C_{15}H_{25}O^+$ $(M + H)^+$, 221.1905; found, 221.1904; **^{1}H NMR** (500 MHz, C_6D_6): δ (ppm) = 5.86 (dd, *J* = 17.5, 10.9 Hz, 1H), 5.18 (t, *J* = 7.3 Hz, 1H), 5.01−4.94 (m, 2H), 4.91 (s, 1H), 4.86 (s, 1H), 4.04 (t, *J* = 8.0 Hz, 1H), 3.95 (t, *J* = 8.0 Hz, 1H), 3.84 (d, *J* = 8.3 Hz, 1H), 3.50 (d, *J* = 8.5 Hz, 1H), 2.37 (t, *J* = 7.4 Hz, 1H), 2.18−2.07 (m, 2H), 2.03−1.91 (m, 2H), 1.66 (s, 3H), 1.53 (s, 3H), 1.05 (s, 3H); **^{13}C NMR** (151 MHz, C_6D_6): δ (ppm) = 147.36, 141.72, 131.54, 124.60, 113.01, 111.28, 78.88, 72.27, 56.13, 48.09, 37.17, 26.94, 25.81, 23.50, 17.72.

Molecular Modeling. All mechanistic based molecular docking studies were performed using MOE 2022.02.[44] The 3D structures of the substrates and intermediates were constructed using "Builder" application in MOE and prepared according to the default protocol of ligand preparation in MOE. The X-ray crystal structures of CotB2 (6GGI),[8] PaFS (5ERM)[16] and TXS (3P5R)[45] have been used for the docking experiment. AlphaFold2[46] was used for structure modeling of PvHVS (uniport id: AZB50511) based on tobacco 5-epi-aristolochene (PDB ID: 5IK9)[47] as a template. The positions of tri-Mg^{2+} ions and GGPP were manually modeled based on the template. All 3D structures were prepared using "Quick Prep" default parameters implemented in MOE. Prior to substrate docking, the active pocket was selected in the receptor molecule where the pyrophosphate of GGPP binds the tri-Mg^{2+} ions. The substrates were docked using "Dock" tool in MOE. For each of the ligands, 1000 poses were taken into consideration according to London dG Score criteria of which the top 100 poses were selected for visualization based on GBVI/WSA dG Score criteria. For all ligands, "Triangle Matcher" was chosen for

https://doi.org/10.1021/acscatal.5c00272
ACS Catal. 2025, 15, 6796−6811

placement, and the "Induced Fit" method was used for refinement of ligand poses, allowing the interaction of flexible side chains at the active site with the substrates.

The final docking pose for each substrate **9**, **10**, **11** was selected from the top 100 poses and evaluated by comparing them to the catalytically competent binding pose of the natural substrate GGPP considering the near attack conformation (NAC) criteria for carbocation formation which should be stabilized through π-system interactions. The NAC geometric criteria are defined for each pose to have ionic interactions between the pyrophosphate group and the tri-Mg^{2+} ion and to posse interatomic distance cyclization about 4.0 Å.[48]

■ ASSOCIATED CONTENT

Supporting Information

The Supporting Information is available free of charge at https://pubs.acs.org/doi/10.1021/acscatal.5c00272.

Detailed chemical procedures, biotransformations and spectral data as well as copies of NMR spectra (PDF)

■ AUTHOR INFORMATION

Corresponding Authors

Mehdi D. Davari − *Department of Bioorganic Chemistry, Leibniz Institute of Plant Biochemistry (IPB), 06120 Halle, Germany;* orcid.org/0000-0003-0089-7156; Email: Mehdi.Davari@ipb-halle.de

Andreas Kirschning − *Institute of Organic Chemistry, Leibniz University Hannover, 30167 Hannover, Germany; Uppsala Biomedical Center (BMC), Uppsala University, 752 37 Uppsala, Sweden;* orcid.org/0000-0001-5431-6930; Email: andreas.kirschning@oci.uni-hannover.de

Authors

Viktoria Ravkina − *Institute of Organic Chemistry, Leibniz University Hannover, 30167 Hannover, Germany*

Gerald Dräger − *Institute of Organic Chemistry, Leibniz University Hannover, 30167 Hannover, Germany*

Jörn Droste − *Institute of Organic Chemistry, Leibniz University Hannover, 30167 Hannover, Germany*

Svenja Schwörer − *Institute of Organic Chemistry, Leibniz University Hannover, 30167 Hannover, Germany*

Ahmed Hassanin − *Department of Bioorganic Chemistry, Leibniz Institute of Plant Biochemistry (IPB), 06120 Halle, Germany; Department of Pharmacognosy, Faculty of Pharmacy, Assiut University, 71256 Assiut, Egypt*

Complete contact information is available at: https://pubs.acs.org/10.1021/acscatal.5c00272

Author Contributions

The manuscript was written through contributions of all authors. All authors have given approval to the final version of the manuscript.

Notes

The authors declare no competing financial interest.

■ ACKNOWLEDGMENTS

We thank Symrise AG (Mühlenfeldstraβe 1, 37603 Holzminden, Germany) for financial support. A.H. is supported by a Ph.D. scholarship from the Ministry of Higher Education of the Arab Republic of Egypt.

■ ABBREVIATIONS

DHP, dihydropyran; *p*TsOH, *p*-toluenesulfonic acid; NCS, *N*-chlorosuccinimide; brsm, based on recovered starting material

■ REFERENCES

(1) Whitehead, J. N.; Leferink, N. G. H.; Johannissen, L. O.; Hay, S.; Scrutton, N. S. Decoding catalysis by terpene synthases. *ACS Catal.* **2023**, *13*, 12774−12802.

(2) Christianson, D. W. Structural and chemical biology of terpenoid cyclases. *Chem. Rev.* **2017**, *117*, 11570−11648.

(3) Baunach, M.; Franke, J.; Hertweck, C. Terpenoid biosynthesis off the beaten track: unconventional cyclases and their impact on biomimetic synthesis. *Angew. Chem., Int. Ed.* **2015**, *54*, 2604−2626.

(4) Harms, V.; Kirschning, A.; Dickschat, J. Nature-driven approaches to non-natural terpene analogues. *Nat. Prod. Rep.* **2020**, *37*, 1080−1097.

(5) Jin, Y.; Williams, D. C.; Croteau, R.; Coates, R. M. Taxadiene synthase-catalyzed cyclization of 6-fluorogeranylgeranyl diphosphate to 7-fluoroverticillenes. *J. Am. Chem. Soc.* **2005**, *127*, 7834−7842.

(6) Cascón, O.; Touchet, S.; Miller, D. J.; Gonzalez, V.; Faraldos, J. A.; Allemann, R. K. Chemoenzymatic preparation of germacrene analogues. *Chem. Commun.* **2012**, *48*, 9702−9704.

(7) Touchet, S.; Chamberlain, K.; Woodcock, C. M.; Miller, D. J.; Birkett, M. A.; Pickett, J. A.; Allemann, R. K. Novel olfactory ligands via terpene synthases. *Chem. Commun.* **2015**, *51*, 7550−7553.

(8) Demiray, M.; Tang, X.; Wirth, T.; Faraldos, J. A.; Allemann, R. K. An efficient chemoenzymatic synthesis of dihydroartemisinic aldehyde. *Angew. Chem., Int. Ed.* **2017**, *56*, 4347−4350.

(9) Tang, X.; Demiray, M.; Wirth, T.; Allemann, R. K. Concise synthesis of artemisinin from a farnesyl diphosphate analogue. *Bioorg. Med. Chem.* **2018**, *26*, 1314−1319.

(10) Huynh, F.; Grundy, D. J.; Jenkins, R. L.; Miller, D. J.; Allemann, R. K. Sesquiterpene Synthase-Catalysed Formation of a New Medium-Sized Cyclic Terpenoid Ether from Farnesyl Diphosphate Analogues. *ChemBioChem* **2018**, *19*, 1834−1838.

(11) Loizzi, M.; Miller, D. J.; Allemann, R. K. Silent catalytic promiscuity in the high-fidelity terpene cyclase δ-cadinene synthase. *Org. Biomol. Chem.* **2019**, *17*, 1206−1214.

(12) Oberhauser, C.; Harms, V.; Seidel, K.; Schröder, B.; Ekramzadeh, K.; Beutel, S.; Winkler, S.; Lauterbach, L.; Dickschat, J. S.; Kirschning, A. Exploiting the synthetic potential of sesquiterpene cyclases for generating unnatural terpenoids. *Angew. Chem., Int. Ed.* **2018**, *57*, 11802−11806.

(13) Harms, V.; Schröder, B.; Oberhauser, C.; Tran, C. D.; Winkler, S.; Dräger, G.; Kirschning, A. Methyl-shifted farnesyldiphosphate derivatives are substrates for sesquiterpene cyclases. *Org. Lett.* **2020**, *22*, 4360−4365.

(14) Tran, C. D.; Dräger, D.; Struwe, H.; Siedenberg, L.; Vasisth, S.; Grunenberg, J.; Kirschning, A. Cyclopropylmethyldiphosphates are substrates for sesquiterpene synthases: experimental and theoretical results. *Org. Biomol. Chem.* **2022**, *20*, 7833−7839.

(15) Harms, V.; Ravkina, V.; Kirschning, A. Mechanistic similarities of sesquiterpene cyclases PenA, Omp6/7, and BcBOT2 are unraveled by an unnatural "FPP-ether" derivative. *Org. Lett.* **2021**, *23*, 3162−3166.

(16) Li, H.; Dickschat, J. S. Diterpene Biosynthesis from Geranylgeranyl Diphosphate Analogues with Changed Reactivities Expands Skeletal Diversity. *Angew. Chem., Int. Ed.* **2022**, *61*, No. e202211054.

(17) Li, H.; Goldfuss, B.; Dickschat, J. S. Enzyme-Catalysed Formation of Hydrocarbon Scaffolds from Geranylgeranyl Diphosphate Analogs with Shifted Double Bonds. *Chem.—Eur. J.* **2025**, No. e202500712.

(18) Kim, S.-Y.; Zhao, P.; Igarashi, M.; Sawa, R.; Tomita, T.; Nishiyama, M.; Kuzuyama, T. Cloning and Heterologous Expression of the Cyclooctatin Biosynthetic Gene Cluster Afford a Diterpene Cyclase and Two P450 Hydroxylases. *Chem. Biol.* **2009**, *16*, 736−743.

(19) Tomita, T.; Kim, S. Y.; Teramoto, K.; Meguro, A.; Ozaki, T.; Yoshida, A.; Motoyoshi, Y.; Mori, N.; Ishigami, K.; Watanabe, H.;

Nishiyama, M.; Kuzuyama, T. Structural Insights into the CotB2-Catalyzed Cyclization of Geranylgeranyl Diphosphate to the Diterpene Cyclooctat-9-en-7-ol. *ACS Chem. Biol.* **2017**, *12*, 1621−1628.
(20) Meguro, A.; Motoyoshi, Y.; Teramoto, K.; Ueda, S.; Totsuka, Y.; Ando, Y.; Tomita, T.; Kim, S.-Y.; Kimura, T.; Igarashi, M.; Sawa, R.; Shinada, T.; Nishiyama, M.; Kuzuyama, T. An unusual terpene cyclization mechanism involving a carbon-carbon bond rearrangement. *Angew. Chem., Int. Ed.* **2015**, *54*, 4353−4356.
(21) Driller, R.; Janke, S.; Fuchs, M.; Warner, E.; Mhashal, A. R.; Major, D. T.; Christmann, M.; Brück, T.; Loll, B. Towards a comprehensive understanding of the structural dynamics of a bacterial diterpene synthase during catalysis. *Nat. Commun.* **2018**, *9*, 3971.
(22) Marra, M.; Camoni, L.; Visconti, S.; Fiorillo, A.; Evidente, A. The Surprising Story of Fusicoccin: A Wilt-Inducing Phytotoxin, a Tool in Plant Physiology and a 14−3-3-Targeted Drug. *Biomolecules* **2021**, *11*, 1393.
(23) Toyomasu, T.; Tsukahara, M.; Kaneko, A.; Niida, R.; Mitsuhashi, W.; Dairi, T.; Kato, N.; Sassa, T. Fusicoccins are biosynthesized by an unusual chimera diterpene synthase in fungi. *Proc. Natl. Acad. Sci. U.S.A.* **2007**, *104*, 3084−3088.
(24) Hezari, M.; Lewis, N. G.; Croteau, R. Purification and characterization of taxa-4(5),11(12)-diene synthase from Pacific yew (*Taxus brevifolia*) that catalyzes the first committed step of Taxol biosynthesis. *Arch. Biochem. Biophys.* **1995**, *322*, 437−444.
(25) Lou, H.; Zheng, S.; Li, T.; Zhang, J.; Fei, Y.; Hao, X.; Liang, G.; Pan, W. Vulgarisin A, a new diterpenoid with a rare 5/6/4/5 ring skeleton from the Chinese medicinal plant Prunella vulgaris. *Org. Lett.* **2014**, *16*, 2696−2699.
(26) Johnson, S. R.; Bhat, W. W.; Sadre, R.; Miller, G. P.; Garcia, A. S.; Hamberger, B. Promiscuous terpene synthases from Prunella vulgaris highlight the importance of substrate and compartment switching in terpene synthase evolution. *New Phytol.* **2019**, *223*, 323−335.
(27) Xu, B.; Tantillo, D. J.; Rudolf, J. D. Mechanistic Insights into the Formation of the 6,10-Bicyclic Eunicellane Skeleton by the Bacterial Diterpene Synthase Bnd4. *Angew. Chem., Int. Ed.* **2021**, *60*, 23159−23163.
(28) Woodside, A. B.; Huang, Z.; Poulter, C. D. Trisammonium geranyl diphosphate. *Org. Synth.* **2003**, *66*, 211.
(29) Williams, D. C.; Wildung, M. R.; Jin, A. Q.; Dalal, D.; Oliver, J. S.; Coates, R. M.; Croteau, R. Heterologous Expression and Characterization of a "Pseudomature" Form of Taxadiene Synthase Involved in Paclitaxel (Taxol) Biosynthesis and Evaluation of a Potential Intermediate and Inhibitors of the Multistep Diterpene Cyclization Reaction. *Arch. Biochem. Biophys.* **2000**, *379*, 137−146.
(30) Chen, M.; Chou, W. K. W.; Toyomasu, T.; Cane, D. E.; Christianson, D. W. Structure and Function of Fusicoccadiene Synthase, a Hexameric Bifunctional Diterpene Synthase. *ACS Chem. Biol.* **2016**, *11*, 889−899.
(31) Nyberg, N. T.; Duus, J. Ø.; Sørensen, O. W. Heteronuclear Two-Bond Correlation: Suppressing Heteronuclear Three-Bond or Higher NMR Correlations while Enhancing Two-Bond Correlations Even for Vanishing 2JCH. *J. Am. Chem. Soc.* **2005**, *127*, 6154−6155.
(32) Nyberg, N. T.; Duus, J. Ø.; Sørensen, O. W. Editing of H2BC NMR spectra. *Magn. Reson. Chem.* **2005**, *43*, 971−974.
(33) Petersen, B. O.; Vinogradov, E.; Kay, W.; Würtz, P.; Nyberg, N. T.; Duus, J. Ø.; Sørensen, O. W. H2BC: a new technique for NMR analysis of complex carbohydrates. *Carbohydr. Res.* **2006**, *341*, 550−556.
(34) Kashman, Y.; Groweiss, A. New diterpenoids from the soft corals Xenia macrospiculata and Xenia obscuronata. *J. Org. Chem.* **1980**, *45*, 3814−3824.
(35) Hong, Y. J.; Tantillo, D. J. The energetic viability of an unexpected skeletal rearrangement in cyclooctatin biosynthesis. *Org. Biomol. Chem.* **2015**, *13*, 10273−10278.
(36) Meguro, A.; Motoyoshi, Y.; Teramoto, K.; Ueda, S.; Totsuka, Y.; Ando, Y.; Tomita, T.; Kim, S.-Y.; Kimura, T.; Igarashi, M.; Sawa, R.; Shinada, T.; Nishiyama, M.; Kuzuyama, T. An unusual terpene cyclization mechanism involving a carbon-carbon bond rearrangement. *Angew. Chem., Int. Ed.* **2015**, *54*, 4353−4356.
(37) Driller, R.; Garbe, D.; Mehlmer, N.; Fuchs, M.; Raz, K.; Major, D. T.; Brück, T.; Loll, B. Current understanding and biotechnological application of the bacterial diterpene synthase CotB2. *Beilstein J. Org. Chem.* **2019**, *15*, 2355−2368.
(38) Kawamura, A.; Iacovidou, M.; Hirokawa, E.; Soll, C. E.; Trujillo, M. 17-Hydroxycyclooctatin, a Fused 5−8−5 Ring Diterpene, from Streptomyces sp. MTE4a. *J. Nat. Prod.* **2011**, *74*, 492−495.
(39) Lee, S. R.; Lee, D.; Park, M.; Lee, J. C.; Park, H.-J.; Kang, K. S.; Kim, C.-E.; Beemelmanns, C.; Kim, K. H. Absolute Configuration and Corrected NMR Assignment of 17-Hydroxycyclooctatin, a Fused 5−8−5 Tricyclic Diterpene. *J. Nat. Prod.* **2020**, *83*, 354−361.
(40) FPP derivative **46** was prepared as reported in ref 12 accept that the hydroxyl group was protected as *tert*-butyldiphenylsilyl ether which allowed better upscaling with improved yields.
(41) Sato, H.; Teramoto, K.; Masumoto, Y.; Tezuka, N.; Sakai, K.; Ueda, S.; Totsuka, Y.; Shinada, T.; Nishiyama, M.; Wang, C.; Kuzuyama, T.; Uchiyama, M. "Cation-Stitching Cascade": exquisite control of terpene cyclization in cyclooctatin biosynthesis. *Sci. Rep.* **2015**, *5*, 18471.
(42) Lauterbach, L.; Goldfuss, B.; Dickschat, J. S. Two Diterpene Synthases from Chryseobacterium: Chryseodiene Synthase and Wanjudiene Synthase. *Angew. Chem., Int. Ed.* **2020**, *59*, 11943−11947.
(43) Nakano, M.; Gemma, R.; Sato, H. Unraveling the role of prenyl side-chain interactions in stabilizing the secondary carbocation in the biosynthesis of variexenol B. *Beilstein J. Org. Chem.* **2023**, *19*, 1503−1510.
(44) Chemical Computing Group ULC. *Molecular Operating Environment (MOE)*; Chemical Computing Group ULC: Montreal, QC, 2022.
(45) Köksal, M.; Jin, Y.; Coates, R. M.; Croteau, R.; Christianson, D. W. Taxadiene synthase structure and evolution of modular architecture in terpene biosynthesis. *Nature* **2011**, *469*, 116−120.
(46) Jumper, J.; Evans, R.; Pritzel, A.; Green, T.; Figurnov, M.; Ronneberger, O.; Tunyasuvunakool, K.; Bates, R.; Žídek, A.; Potapenko, A.; Bridgland, A.; Meyer, C.; Kohl, S. A. A.; Ballard, A. J.; Cowie, A.; Romera-Paredes, B.; Nikolov, S.; Jain, R.; Adler, J.; Back, T.; Petersen, S.; Reiman, D.; Clancy, E.; Zielinski, M.; Steinegger, M.; Pacholska, M.; Berghammer, T.; Bodenstein, S.; Silver, D.; Vinyals, O.; Senior, A. W.; Kavukcuoglu, K.; Kohli, P.; Hassabis, D. Highly accurate protein structure prediction with AlphaFold. *Nature* **2021**, *596*, 583−589.
(47) Koo, H. J.; Vickery, C. R.; Xu, Y.; Louie, G. V.; O'Maille, P. E.; Bowman, M.; Nartey, C. M.; Burkart, M. D.; Noel, J. P. Biosynthetic potential of sesquiterpene synthases: product profiles of Egyptian Henbane premnaspirodiene synthase and related mutants. *J. Antibiot.* **2016**, *69*, 524−533.
(48) Tomita, T.; Kim, S.-Y.; Teramoto, K.; Meguro, A.; Ozaki, T.; Yoshida, A.; Motoyoshi, Y.; Mori, N.; Ishigami, K.; Watanabe, H.; Nishiyama, M.; Kuzuyama, T. Structural Insights into the CotB2-Catalyzed Cyclization of Geranylgeranyl Diphosphate to the Diterpene Cyclooctat-9-en-7-ol. *ACS Chem. Biol.* **2017**, *12*, 1621−1628.

https://doi.org/10.1021/acscatal.5c00272
ACS Catal. 2025, 15, 6796−6811